Organic Geochemistry 83–84 (2015) 178–189

Contents lists available at ScienceDirect

Organic Geochemistry

journal homepage: www.elsevier.com/locate/orggeochem

Hydrogen isotope characteristics of thermogenic methane in Chinese sedimentary basins

Xiaofeng Wang [a,*], Wenhui Liu [b], Baoguang Shi [a], Zhongning Zhang [a], Yongchang Xu [a], Jianjing Zheng [a]

[a] *Key Laboratory of Petroleum Resources, Gansu Province/Key Laboratory of Petroleum Resources Research, Institute of Geology and Geophysics, Chinese Academy of Sciences, Lanzhou 730000, China*

[b] *Institution of Petroleum Exploration and Development, SINOPEC, Beijing 100083, China*

ARTICLE INFO

Article history:
Received 9 April 2014
Received in revised form 13 March 2015
Accepted 13 March 2015
Available online 20 March 2015

Keywords:
Natural gas
Hydrogen isotope
Thermogenic methane
Chinese sedimentary basins

ABSTRACT

The hydrogen isotope composition of methane is an important parameter in natural gas research and provides complementary information to that provided by carbon isotopes. The stable hydrogen isotope ratios of 313 natural gas samples from six of China's sedimentary basins are used to evaluate the factors that influence the stable hydrogen isotopic composition of methane. An important factor is the δD of organic matter in hydrocarbon source rocks, which is influenced by the sedimentary environment and type of organic matter. Natural gases generated from sapropelic organic matter have relatively less negative δD_{CH_4}, while natural gases generated from humic organic matter have relatively more negative δD_{CH_4}. The other factor is thermal maturity. Increased thermal maturity leads to δD_{CH_4} becoming less negative and there exists a two stage linear relationship between the δD_{CH_4} and the logarithm of the vitrinite reflectance (*Ro*) value for natural gases generated from type III kerogen. The third factor is the environmental conditions of the aqueous medium in the original depositional environment and after sedimentation. Elemental hydrogen from water participates in biochemical processes as organisms grow and is exchanged during the sedimentation and diagenesis of organic matter as well as maturity process of kerogen to generate gases. The influence of the aqueous medium on δD_{CH_4} after formation of natural gases can be ignored. Among these factors, the aqueous medium is the key constraining factor. The δD_{CH_4} in natural gases can be combined with the use of stable carbon isotopic composition to identify the origins of natural gases and to aid gas-source correlations.

© 2015 Elsevier Ltd. All rights reserved.

1. Introduction

Methane and its stable carbon isotopic composition ($\delta^{13}C_{CH_4}$) are of wide concern in studying the origin of natural gas because methane is the main component of the hydrocarbon gases in natural gas. Values of $\delta^{13}C_{CH_4}$ are a useful diagnostic tool in identifying the origins of natural gases and gas-source correlations (Stahl and Carey, 1975; Stahl et al., 1977; Schoell, 1980, 1983, 1984, 1988; Whiticar et al., 1986; Whiticar, 1999; Dai, 1992; Xu, 1994; Liu et al., 2007). Hydrogen, the other element of methane, composed of ^1H and deuterium (^2H or D) stable isotopes, has the largest isotopic mass difference of any stable isotope pair (Bigeleisen, 1965). This results in a wide range of the δD_{CH_4} in nature (−470‰ to −16‰; Dai, 1993). Since the pioneering work of Schoell (1980), δD_{CH_4} has been used widely in studies of biogenic gas sources (Whiticar et al., 1986; Whiticar, 1999). Whiticar (1999) proposed that hydrogen isotope effects during methanogenesis of methylated substrates can lead to D depletion as large as δD_{CH_4} = −531‰ VSMOW, whereas bacterial hydrogen isotope fractionation for the CO_2 reduction pathway is significantly less (δD_{CH_4} = −250‰ to −170‰).

Li et al. (2001) proposed that the δD values of alkanes in crude oils are determined by three factors, including the isotopic compositions of the biosynthetic precursors, source water δD values and post-depositional processes. Sessions et al. (1999) have established that the isotopic compositions of biosynthetic precursors, fractionation and isotope exchange accompanying biosynthesis and hydrogenation during biosynthesis are all important in determining hydrogen isotope abundance. However, hydrogen isotope research on the origins of thermogenic natural gases is relatively delayed compared with carbon isotope because hydrogen isotope analytical techniques were not sophisticated or online and the factors influencing the δD in thermogenic natural gases were insufficiently understood. In the late 1990s, the application of gas chromatography–thermal conversion–isotope

* Corresponding author. Tel./fax: +86 931 4960853.
E-mail address: wangxf@lzb.ac.cn (X. Wang).

http://dx.doi.org/10.1016/j.orggeochem.2015.03.010
0146-6380/© 2015 Elsevier Ltd. All rights reserved.

ratio mass spectrometry made online analysis of the δD in natural gases possible (Hilkert et al., 1999; Shouakar et al., 2000; Dai et al., 2012a). The $\delta^{13}C$ and δD values can be combined for problem solving in oil and gas exploration.

2. Samples and experiments

Geochemical data for 313 gas samples from six of China's sedimentary basins are used in this study, including literature data for 112 samples and additional data for 201 samples collected specifically for this study. All gas samples were analyzed in the Key Laboratory of Petroleum Resources Research, Institute of Geology and Geophysics, Chinese Academy of Sciences at Lanzhou.

Compound specific hydrogen stable isotope ratios were determined using a Finnigan Mat Delta Plus mass spectrometer interfaced with a HP 5890II gas chromatograph. In this method, online hydrogen isotope analysis was achieved for oil and natural gas hydrocarbons. Gas components were separated on a HP-PLOT Q column (30 m × 0.32 mm × 20 μm) with helium as the carrier gas (1.5 ml/min). A split injection was used for methane with a split ratio of 1:7 at 40 °C. Ethane and propane were introduced via splitless injection. The GC oven temperature was initially 40 °C for 4 min, then increased to 80 °C at 10 °C/min, then to 140 °C at 5 °C/min and finally to 260 °C at 30 °C/min. Natural gas was separated into its constituent hydrocarbons by gas chromatography and these entered the high temperature conversion interface at 1450 °C and were decomposed into C and H_2. The C was bound in the furnace and H_2 entered the isotope mass spectrometer for δD analysis. Relatively high measurement precision was due to no requirement of zinc or uranium reduction. Gas samples were analyzed in duplicate or triplicate when the content of C_2–C_5 was very low. The precision was ± 3‰ with respect to VSMOW.

Compound specific stable carbon isotope ratios were determined using a Finnigan Mat Delta Plus mass spectrometer interfaced with a HP 5890II gas chromatograph. Gas components were separated on the gas chromatograph using helium as the carrier gas, converted into CO_2 in a combustion interface and then introduced into the mass spectrometer. Individual hydrocarbon gas components (C_1–C_5) and CO_2 were initially separated using a fused silica capillary column (PLOT Q 30 m × 0.32 mm). The GC oven temperature was increased from 35 °C to 80 °C at 8 °C/min, then to 260 °C at 5 °C/min and held at 260 °C for 10 min. Gas samples were analyzed in duplicate or triplicate if the content of C_2–C_5 was very low. Stable isotope ratios for carbon are reported in δ notation in permil (‰) relative to VPDB. The measurement precision was estimated to be ± 0.5‰ for $\delta^{13}C$.

Gas chemical compositions were determined on an Agilent 6890N gas chromatograph equipped with a flame ionization detector and a thermal conductivity detector. Individual hydrocarbon gas components from C_1 to C_5 were separated using a capillary column (PLOT Al_2O_3 50 m × 0.53 mm). The GC oven temperature was initially held at 30 °C for 10 min and then increased to 180 °C at 10 °C/min and held at this temperature for 20–30 min.

3. Results and discussion

3.1. Experimental results

The chemical compositions and stable carbon/hydrogen isotope composition of 313 natural gas samples are listed in Appendix A. The C_2–C_3 isotope compositional data was not available for some gas samples because of low concentrations. The δD ranges for methane, ethane and propane were −271‰ to −111‰ (mean −188‰), −249‰ to −105‰ (mean −164‰) and −237‰ to −75‰ (mean −151‰), respectively.

Hydrogen isotope tends to become heavier with the increasing carbon number in typical thermogenic gases. That is, it has a positive sequence distribution characteristic in hydrogen isotopes ($\delta D_{CH_4} < \delta D_{C_2H_6} < \delta D_{C_3H_8}$) (Barker and Pollock, 1984; Dai, 1993). However, the normal sequence of hydrogen isotopes could be inverted in some situations (Dai, 1993). First, the δD values can be changed by biodegradation and oxidation and C–H bonds are oxidized more easily than C–D bonds due to the lower energy of C–H bonds (Coleman and Risatti, 1981). For example, propane molecule with a C–H bond is preferentially degraded and this leads the δD of the residual propane to become more positive. Second, the normal sequence of hydrogen isotopes can be changed by the mixture of different types of gases (Dai, 1990, 1993). The experimental result shows that D enrichment occurred as *n*-alkanes increased in length (Fig. 1). For some samples in the Tarim Basin, the δD values of the alkane gases showed the opposite sequence ($\delta D_{CH_4} > \delta D_{C_2H_6}$ or $\delta D_{C_2H_6} > \delta D_{C_3H_8}$), where this may be caused by mixing of natural gases. It shows a similar sequence of carbon isotopes compared with hydrogen isotopes, a reversal or a partial reversal of $\delta^{13}C_{CH_4}$ was observed in the samples from Tarim Basin (Fig. 1E).

3.2. Factors influencing the hydrogen isotope composition of natural gases

Because the carbon in thermogenic natural gases is single source, the influencing factors of $\delta^{13}C_{CH_4}$ are mainly type of organic matter in the source rocks and thermal maturity. Natural gases derived from the same type of organic matter show an obvious corresponding relation between the reflectance of vitrinite (*Ro*) and $\delta^{13}C_{CH_4}$ and this relationship plays an important role in gas-source correlations (Stahl and Carey, 1975; Stahl et al., 1977; Schoell, 1983; Liu and Xu, 1999). Compared with $\delta^{13}C_{CH_4}$, the factors influencing the δD in natural gases are more complex. The δD_{CH_4} value increases with increasing maturity (Schoell, 1980; Dai, 1993). In addition, the type of organic matter, sedimentary environment and conditions in the aqueous medium may influence the δD of natural gases.

3.2.1. Effect of inheritance

The δD_{CH_4} of the natural gas is primarily determined by the δD of the organic matter in the source rocks and the δD of the organic matter is determined by the sedimentary environment and the type of organic matter. Biochemical reactions tend to enrich H so that different organisms have different δD characteristics. Generally, organisms partly inherit the δD characteristics from host water. Organisms are depleted in D compared with the host water (Whiticar, 1996) and higher δD values in the aqueous media result in higher δD values for the organisms. Additionally, the δD values of aqueous media are related to salinity, higher salinity of aqueous media leads to D enrichment because of Rayleigh fractionation caused by evaporation. Therefore, aquatic organisms are more enriched in D than terrigenous organisms and marine organisms are more enriched in D than freshwater lacustrine organisms.

Hydrocarbon source rocks inherit the δD characteristics from organisms. Hydrocarbon source rocks formed in marine and saline lacustrine environments are relatively enriched in D, while those formed in terrigenous freshwater are relatively depleted in D. The inherited δD characteristics are reflected in the δD_{CH_4} values of thermogenic natural gases. For example, for natural gases of the same maturity, those derived from marine and saline water lacustrine hydrocarbon source rocks (generally type I and type II_1 organic matter) are enriched in D compared with those derived

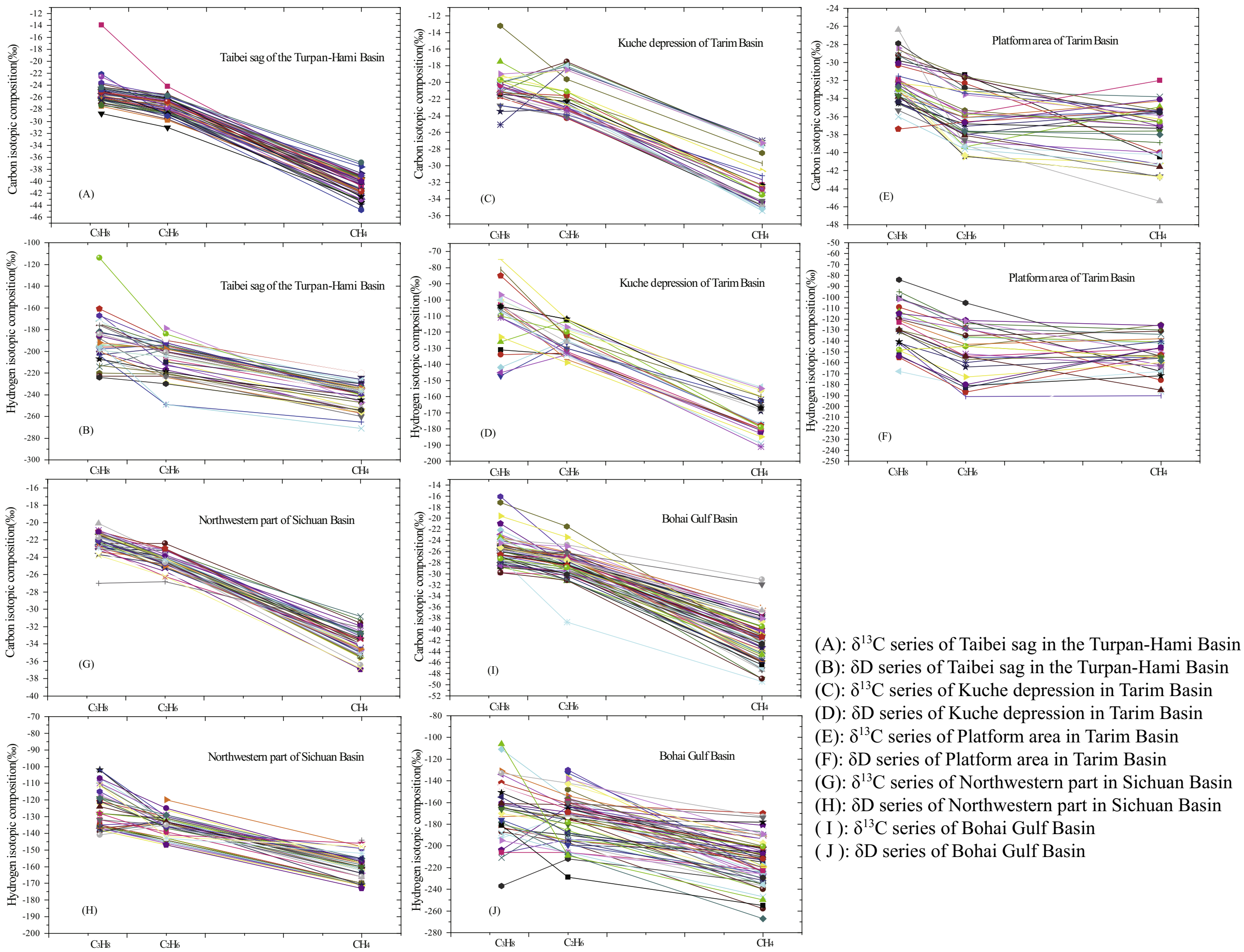

Fig. 1. Plot of C and H isotope composition of methane, ethane and propane versus the reciprocal C number of gas samples. D enrichment occurred as the amount of paraffin increased in thermogenic methane of Chinese sedimentary basins. The hydrogen isotope distribution characteristics of alkane gases is similar to that of the carbon isotopes.

from freshwater lacustrine and freshwater swamp facies hydrocarbon source rocks (generally type II_2 and type III organic matter). Shen and Xu (1993) suggested a δD_{CH_4} value of −190‰ to discriminate depositional environments, natural gases from marine source rocks show δD_{CH_4} > −190‰ and gases from terrigenous freshwater sources show δD_{CH_4} < −190‰. However, this value is unsuitable because some highly mature gases from terrigenous freshwater sources have δD_{CH_4} values less negative than −150‰, such as natural gases from the northwestern Sichuan Basin.

3.2.2. Thermal maturity

Schoell (1980) found that the bond energy of the C–C bond of R-CH_2D in parent material of hydrocarbons is much higher than that of the C–C bond of R-CH_3. As a result, the C–CH_2D bond cleavage reactions happened when thermal stress increased to a fairly high level. So D is enriched in methane gradually with the maturity increase. Schoell (1980) developed the equation $\delta D_{CH_4} = 35.5 \log Ro - 152$ (‰). Nevertheless, there is a relatively large difference in the relationship between the δD_{CH_4} and the thermal maturity as indicated by the *Ro* of vitrinite because source rocks contain different types of organic matter. Thus the model has not found wide application.

The δD_{CH_4} values obtained for samples from China's typical coal-type gas fields range from −271‰ to −142‰ (Fig. 2). There

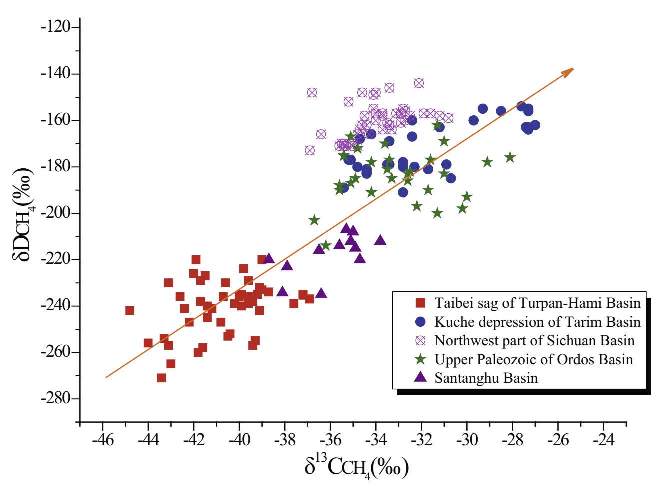

Fig. 2. Plot of H isotope composition of methane in natural gases from typical coal-type gas fields in China versus C isotope values. Note the positive linear relationship between the $\delta^{13}C_{CH_4}$ and δD_{CH_4} in the natural gases.

was a linear relationship between the $\delta^{13}C_{CH_4}$ and the δD_{CH_4} values for these samples. This relationship between $\delta^{13}C$ and the δD can be expressed as δD_{CH_4} (‰) = $5.6247\delta^{13}C_{CH_4} + 3.013$‰ ($R^2 = 0.82$,

$n = 97$). The relationship between $\delta^{13}C_{CH_4}$ and δD_{CH_4} in coal-type gases from the northwestern Sichuan Basin deviate from this equation and this may be explained by the aqueous medium conditions of the gas source rocks as discussed below.

A series of models have been proposed for the relationship between $\delta^{13}C_{CH_4}$ and the *Ro*. Liu and Xu (1999) established a two-stage model for the $\delta^{13}C_{CH_4}$ from typical coal-type gas fields in China and this model has found wide application in China (Xu et al., 2006; Shi et al., 2012). According to this model, the following equations can be obtained for the δD_{CH_4} values:

$$\delta D_{CH_4}\ (‰) = 289.99 \lg Ro - 183.58\ R^2 = 0.7371\ (Ro < 1.0\%),\ n = 50,$$
$$\delta D_{CH_4}\ (‰) = 55.71 \lg Ro - 182.22\ R^2 = 0.5027\ (Ro > 1.0\%),\ n = 47.$$

It shows that the δD_{CH_4} change with *Ro* can be divided into two phases: the δD_{CH_4} increases rapidly when *Ro* is less than 1% and the increasing rate of δD_{CH_4} is slow when *Ro* exceeds 1% (Fig. 3). Generally, the dryness index of natural gas is related to the maturity. The relationship between the gas dryness index and δD_{CH_4} indicate that δD_{CH_4} becomes less negative as the gas dryness index increases (Fig. 4). This suggests that δD_{CH_4} is also influenced by maturity.

3.2.3. Aqueous medium conditions

The aqueous medium is an important factor in determining the δD_{CH_4}. It is involved in the entire process from organism to natural gas and influences the hydrogen isotope composition of methane. The influencing mechanism is embodied in three aspects. Firstly, the δD of the organism is influenced by aqueous medium and this is reflected in the δD of sedimentary organic matter. Secondly, the δD of kerogen is influenced by the aqueous medium conditions from deposition to diagenesis. Finally, the aqueous medium conditions during the process of gas generation from kerogen, influence the hydrogen isotope composition of methane. Generally, hydrogen isotope exchange between gaseous hydrocarbon and water is very slow under natural conditions. At temperatures of 200–240 °C over one hundred million years, the δD_{CH_4} has hardly changed (Yeh and Epstein, 1981; Schoell, 1984; Schimmelmann et al., 2001). Therefore, the influence of the aqueous medium on δD after formation of natural gases can be ignored.

During the process from sedimentation to diagenesis, the aqueous medium conditions influence the δD of kerogen by hydrogen isotope exchange reaction between the aqueous medium and the organic matter. Rapid reversible hydrogen isotope exchange reactions can occur between hydrogen in the water and hydrogen in the sedimentary organic matter that is bound to heteroatoms (i.e. N–H, S–H, O–H) (Schimmelmann et al., 1999, 2001). Hydrogen atoms on alkyl radicals in sedimentary organic matter can preserve their original hydrogen isotope composition until the temperature rises above 150 °C (Lewan, 1997; Schimmelmann et al., 1999; Mastalerz and Schimmelmann, 2002). Therefore, the hydrogen isotope composition has been less influenced by the process from sedimentation to diagenesis.

Wang et al. (2008, 2011) performed coal pyrolysis experiments with deionized water ($\delta D_{H_2O} = -58‰$) and seawater ($\delta D_{H_2O} = -4.8‰$). The gas produced with deionized water was depleted in deuterium compared to the gas produced with seawater (Fig. 5) and the average difference between values from two experiments was 20‰. This indicates that the δD characteristics of paleo-aqueous media during the natural gas formation have some influence on the δD of natural gases.

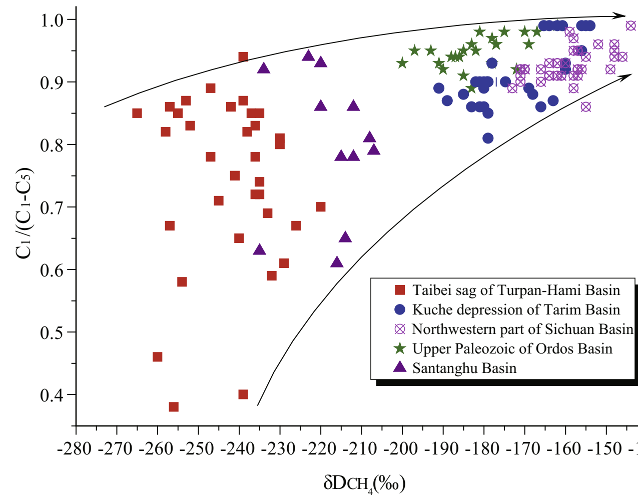

Fig. 4. Relationship between the gas dryness index and δD_{CH_4} in typical coal-type natural gases in Chinese sedimentary basins.

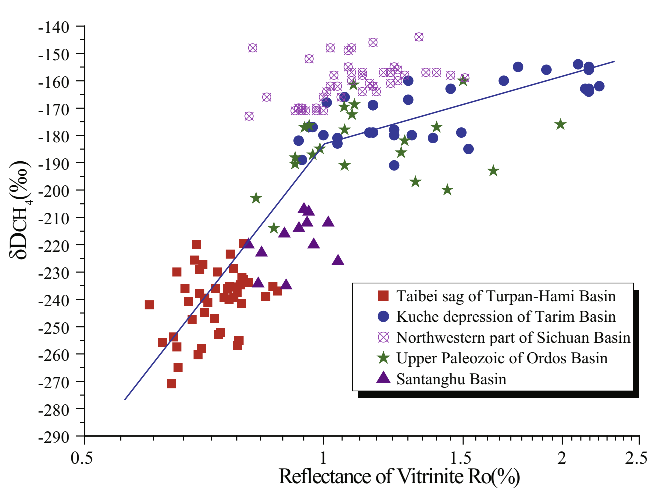

Fig. 3. Two-stage model of δD_{CH_4} and the *Ro* in typical coal-type natural gases in Chinese sedimentary basins. The *Ro* is calculated by the "two-stage model" for $\delta^{13}C_{CH_4}$ in China's typical coal-type gas fields (Liu and Xu, 1999).

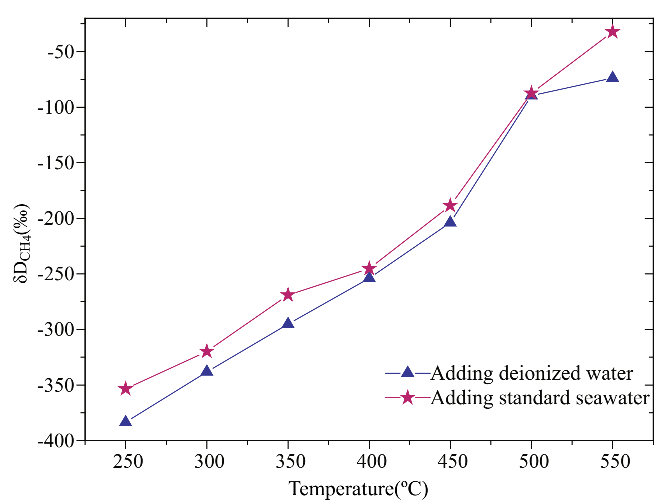

Fig. 5. The role of water in chemical reactions during hydrocarbon generation and its influence on the hydrogen isotopic composition of methane. Note that the hydrogen isotopic composition of the methane produced in the seawater-added experiments were enriched in D compared to that in the deionized water-added experiments.

The relationship between the $\delta^{13}C_{CH_4}$ and δD_{CH_4} in coal-type gases from six basins in China are shown in Fig. 2. The sedimentary environments of the gas source rocks in the basins are dominantly terrigenous freshwater except Sichuan Basin. It shows an evidently linear relationship between the $\delta^{13}C_{CH_4}$ and δD_{CH_4} in the coal-type gases from basins except Sichuan Basin. By contrast, the coal-type gas samples from the Sichuan Basin obviously deviate from the linear relationship and the δD_{CH_4} values are less negative.

The coal-type gas samples from the Sichuan Basin are located in the northwest of the basin and the gas source rocks are coal series strata of transitional facies in the Triassic Xujiahe Formation (Zhang et al., 2009; Dai et al., 2012b). The Xujiahe Formation sedimentary strata are indicative of a transformation from a marine high salinity water to terrigenous low salinity water. In the sedimentation stages of the Xujiahe Formation, stages Xu-1 to Xu-4 occurred under relatively high paleosalinity with lower values for Xu-5 and Xu-6 indicative of a terrigenous environment (Lin et al., 2006; Jin et al., 2010). Consequently, in northwest Sichuan Basin, the enrichment of D in the coal-type gases can be caused by the high paleosalinity of the water body in which the hydrocarbon source rocks were deposited.

Additionally, alteration after formation of the natural gas reservoirs may also influence the δD values of the natural gases, including natural gas mixing, bacterial transformation and thermochemical sulfate reduction.

3.3. Hydrogen isotope geochemical characteristics of China's natural gases and their geological implications

Fig. 6 shows statistical data for the δD characteristics of the natural gas samples collected from six sedimentary basins of China. The geological background data for these basins are given in Table 1. Natural gases in the Taibei sag of the Turpan-Hami Basin are immature coal-type gases (Xu et al., 2006, 2009; Dai et al., 2009) and the hydrocarbon source rocks are freshwater swamp-facies coal-series rocks of Middle-Lower Jurassic. The *Ro* of these hydrocarbon source rocks are mainly between 0.4% and 0.9%. The δD_{CH_4} values in this region are range from −271‰ to −220‰, that is, they are relatively depleted in D. Natural gases in the Santanghu Basin are distributed in the Malang sag. The gas source rocks are dark colored mudstone and coal of Upper Carboniferous. The sedimentary environment of the Upper Carboniferous is dominantly terrigenous and the paleo-aqueous media are generally represented by freshwater. In this basin, the *Ro* is mainly between 0.5% and 1.6% and the δD_{CH_4} values are range from −235‰ and −207‰. This indicates that the natural gases from the Santanghu Basin are slightly enriched in D compared with those from the Turpan-Hami Basin.

The Upper Paleozoic natural gases in the Ordos Basin are high maturity coal-type gases and their δD_{CH_4} are range from −214‰ to −162‰ (average −184‰). The source rocks of this gas field are carbonaceous mudstone and coal measures formed in the Upper Paleozoic peat bog system. The organic matter of the source rocks is dominated by types II_2–III and the paleo-aqueous media are dominantly freshwater. The δD values for Upper Paleozoic natural gases from the Ordos Basin are slightly more enriched in D than those for the coal-type gases from the Santanghu Basin.

Natural gases in the Kuche depression of the Tarim Basin are over mature coal-type gases and the hydrocarbon source rocks are freshwater swamp facies, coal series rocks of Triassic-Jurassic. The *Ro* values are between 1.0% and 2.2% (Qin et al., 2007) and the δD_{CH_4} in the natural gases are range from −191‰ to −154‰, which indicates that the samples are especially enriched in D.

Natural gases in the regions mentioned above are all typical coal-type gases. The organic matter of gas source rocks are mainly humic type (type III) and the sedimentary aqueous media are dominantly freshwater. It yielded a significant positive linear relationship between the $\delta^{13}C_{CH_4}$ and δD_{CH_4} of the natural gases (Fig. 2).

Natural gases mainly from the Xinchang gas field, which located in the northwest of the Sichuan Basin, are mature coal-type gases. The Xujiahe Formation hydrocarbon source rocks contain type III organic matter. Because the sedimentary environment of Xujiahe Formation is dominantly saline water (Lin et al., 2006; Jin et al., 2010), the δD_{CH_4} of the natural gases are relatively less negative with a range of −173‰ to −144‰. These results deviate from the linear relationship between the $\delta^{13}C_{CH_4}$ and δD_{CH_4} in natural gases derived from typical freshwater swamp facies, coal series hydrocarbon source rocks, indicating that the salinity of aqueous media can influence the δD of natural gases.

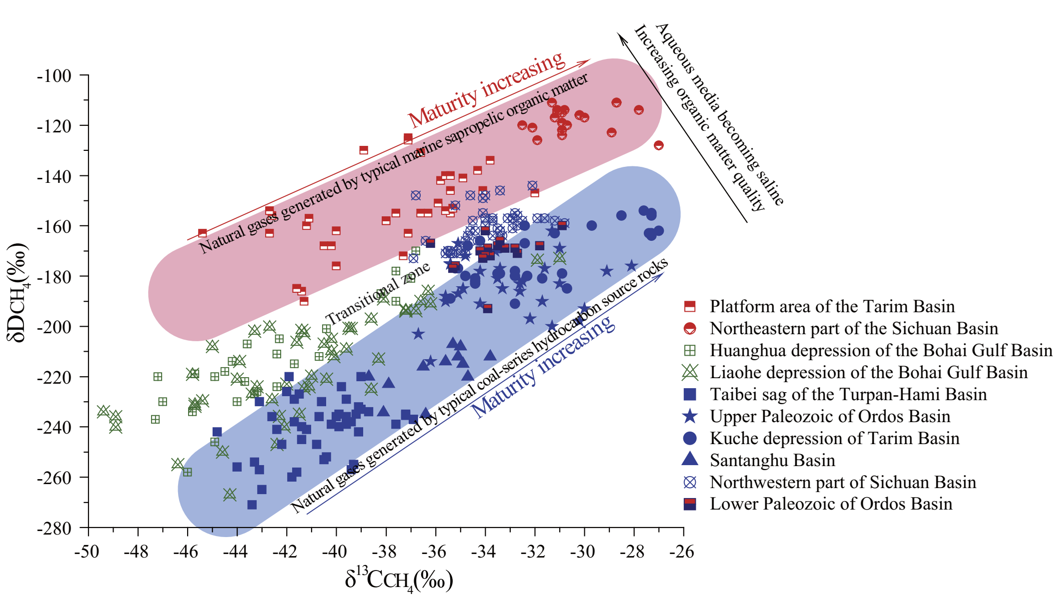

Fig. 6. Plot of δD_{CH_4} versus $\delta^{13}C_{CH_4}$ for thermogenic methane in Chinese sedimentary basins. The influence of factors affecting δD_{CH_4} is greater than on $\delta^{13}C_{CH_4}$, in addition to maturity and hydrocarbon source characteristics. Aqueous media is also a very important factor.

Table 1
Geological background of natural gas reservoirs in Chinese sedimentary basins.

Region	Hydrocarbon source rocks	Sedimentary facies of hydrocarbon-source rocks	Salinity of sedimentary waterbody	Characteristics of hydrocarbon source rocks	Natural gas type	δD_{CH_4} (‰)	$\delta^{13}C_{CH_4}$ (‰)	$\delta^{13}C_{C_2H_6}$ (‰)
Taibei sag of the Turpan-Hami Basin	$J_{1+2}sh$	Terrestrial swamp	Freshwater	Coal series, type III organic matter, *R*o = 0.4% to 0.9%	Low mature coal-type gas	−271 to −220/ −241 (46)	−44.8 to −36.9/ −40.7 (46)	−31.0 to −24.2/ −27.5 (46)
Santanghu Basin	C	Marine/ terrestrial transition-facies	Freshwater	Dark mudstone and coal, type II_2–III organic matter, *R*o = 0.5% to 1.6%	Mature coal-type gas	−235 to −207/ −218 (12)	−38.7 to −33.8/ −36.0 (12)	−28.5 to −23.6/ −27.0 (12)
Upper Paleozoic of Ordos Basin	C + P	Marine/ terrestrial transition-facies	Freshwater	Coal and dark mudstone, type II_2–III organic matter, *R*o = 0.7% to 2.0%	Mature-highly mature coal-type gas	−214 to −162/ −184 (29)	−36.7 to −28.1/ −33.0 (29)	−29.3 to −20.8/ −25.0 (29)
Lower Paleozoic of Ordos Basin	O?	Marine facies	Saline water	Carbonate rock, type I organic matter, *R*o = 1.0% to 3.0%	Mixture?	−193 to −160/ −171 (17)	−36.2 to −30.9/ −33.7 (17)	−34.1 to −23.7/ −29.0 (17)
Kuche Depression of Tarim Basin	T + J	Terrestrial-facies swamp	Freshwater	Coal series, type III organic mater, *R*o = 1.0% to 2.2%	Mature-highly mature coal-type gas	−191 to −154/ −172 (32)	−35.4 to −27.0/ −31.7 (32)	−24.3 to −17.5/ −21.7 (32)
Northwestern part of Sichuan Basin	T_3x	Marine/ terrestrial transition facies	Saline water	Coal series, type III organic matter, *R*o = 0.8% to 2.6%	Mature-highly mature coal-type gas	−173 to −144/ −160 (46)	−36.9 to −30.8/ −34.0 (46)	−26.8 to −22.4/ −24.4 (46)
Platform Area of the Tarim Basin	∈ + O	Marine facies	Saline water	Carbonate rock, type I organic matter, *R*o = 1.0% to 3.0%	Highly mature-over mature oil-type gas	−190 to −125/ −154 (37)	−45.4 to −32.0/ −37.9 (37)	−41.8 to −31.4/ −36.4 (37)
Northeastern part of the Sichuan Basin	S	Marine facies	Saline water	Black shale, type I organic matter, *R*o ≈ 2.5% to 3.5%	Over mature oil-type gas	−128 to −111/ −118 (19)	−32.5 to −27.0/ −30.5 (19)	−32.2 to −24.0/ −29.5 (19)
Huanghua depression of the Bohai Gulf Basin	Es	Lacustrine facies	Semi-saline water	Dark mudstone, organic matter type is complicated and diverse, type II and type III organic matter being dominant	Low mature coal-type gas	−258 to −170/ −215 (26)	−47.3 to −36.8/ −42.8 (26)	−31.3 to −21.5/ −28.2 (26)
Liaohe depression of the Bohai Gulf Basin	Es	Lacustrine facies	Brackish water	Dark mudstone, organic matter type is complicated and diverse, type II and type III organic matter being dominant	Mainly composed of low mature coal-type gas	−267 to −173/ −216 (49)	−49.4 to −31.0/ −41.4 (49)	−38.7 to −23.4/ −28.0 (49)

Remarks: in $a \sim b/c\ (d)$ pattern, *a* represents the minimum value, *b* represents the maximum value, *c* represents the average value, *d* represents the number of samples.

A series of gas fields have been discovered in the Liaohe depression and Huanghua depression of the Bohai Gulf Basin in eastern China. The characteristics of the Shahejie Formation hydrocarbon source rocks are complicated and diversified, but organic matter is dominantly mixed type (II) and humic type (III) kerogen. The hydrocarbon source rocks in most regions have relatively low thermal maturity (*R*o < 1.0%). Hydrocarbon source rocks in the Liaohe depression are mainly deposited in fresh water and brackish water, while those in the Huanghua depression are deposited in semi-saline water. The $\delta^{13}C_{CH_4}$ values in natural gases from two regions are relatively more negative, but the $\delta^{13}C$ values of ethane are relatively less negative. The carbon stable isotope composition are generally consistent with those of natural gases from the Turpan-Hami Basin, which shows the characteristics of immature coal-type gases and the δD_{CH_4} values are relatively more negative. As shown in Fig. 6, the $\delta^{13}C_{CH_4}$ and δD_{CH_4} values in some gas samples from the Liaohe depression are generally consistent with the linear relationship of natural gases generated from typical freshwater swamp facies, coal series hydrocarbon source rocks. However, the δD_{CH_4} values in some natural gas samples are slightly less negative and deviate from this linear relationship. The relationship between the $\delta^{13}C_{CH_4}$ and δD_{CH_4} values in natural gases from the Huanghua depression obviously deviates from that for the natural gases generated from typical freshwater swamp facies, coal series hydrocarbon source rocks, this may be attributed to the fact that the sedimentary water body of hydrocarbon source rocks is relatively saline (Lin, 2011).

The natural gases of the northeastern part of the Sichuan Basin and platform area of the Tarim Basin are generated from typical marine hydrocarbon-source rocks. Their δD_{CH_4} values are less negative (−190‰ and −111‰) than that generated from terrigenous hydrocarbon source rocks. It shows a linear relationship between the $\delta^{13}C_{CH_4}$ and δD_{CH_4} values with both becoming less negative with increasing maturity (Fig. 6). The δD_{CH_4} of marine natural gases in the Tarim Basin were range from −190‰ to −125‰, which indicates that the natural gases are high maturity, oil associated gases, which is consistent with high maturity Cambrian-Ordovician marine carbonate source rocks. The δD_{CH_4} values in marine natural gases from the northeastern Sichuan Basin are relatively less negative (−128‰ and −111‰), which indicates that the natural gases are over mature, oil associated gases.

Many studies have been carried out in Ordos Basin since the Central Gas Field was found in this area. However, the gas source rocks of the Central Gas Field are a problem that is not completely solved. It is generally accepted that natural gases from the Upper Paleozoic gas generating layers are dominated by coal derived gases. Nevertheless, the origin of Lower Paleozoic Ordovician weathering crust is controversial. It is generally thought that these natural gases are two-source mixture of coal generated gases by Upper Paleozoic and oil associated gases by Lower Paleozoic, but the dominant gas source is still controversial. Some argue that natural gases in the Ordovician weathering crust of the Central Gas Field are mainly derived from Carboniferous-Permian coal series hydrocarbon source rocks (Guan et al., 1993; Zhang et al., 1993; Dai et al., 2005; Hu et al., 2010), whereas others maintain that natural gases in the Ordovician weathering crust are mainly derived from the Lower Paleozoic marine carbonate rocks (Chen, 1994; Huang et al., 1996; Hao et al., 1997; Cai et al., 2005; Liu et al., 2009).

$\delta^{13}C_{CH_4}$ values are unable to constrain the origin of natural gases because the range of $\delta^{13}C_{CH_4}$ values in Lower Paleozoic and Upper Paleozoic natural gases are overlapping. The evidence for the derivation of Lower Paleozoic natural gases mainly from Ordovician hydrocarbon source rocks includes the $\delta^{13}C$ of ethane, parameters for light hydrocarbon compounds and the parameters for biomarker compounds of natural gases. But the C_2–C_5 contents are generally lower than 1% in Lower Paleozoic natural gases and the contents of light hydrocarbon compounds and biomarker compounds are even lower. Therefore, the geochemical parameters for this kind of trace gas in natural gases used to constrain the origin of natural gases may lead to an incorrect interpretation.

The hydrogen stable isotope compositions of methane in Lower Paleozoic natural gases from the Ordos Basin are range from −193‰ to −160‰ and the average value is −170‰ (Li et al., 2008). The average value is obviously less negative than that of methane in the Upper Paleozoic natural gases (−191‰, Fig. 6), which indicates that the Lower Paleozoic natural gases in the Ordos Basin derived from a mixed source and Lower Paleozoic marine carbonate rocks have made some contributions to hydrocarbon generation. However, the average value of δD_{CH_4} is quite different compared with the values of natural gases derived from typical marine sapropelic organic matter in China. It shows that the Lower Paleozoic natural gases are derived from Carboniferous-Permian coal series and mixed with a minor amount of gas generated from Lower Paleozoic marine carbonate rocks.

The δD_{CH_4} values in natural gases are closely related to the sedimentary environment and the $\delta^{13}C$ of ethane in natural gases is a reflection of the type of organic matter. The relationship between the δD_{CH_4} and the $\delta^{13}C$ values of ethane in natural gases from China are shown in Fig. 7. The Lower Paleozoic natural gases in the Ordos Basin lie in the range between natural gases generated from marine sapropelic organic matter and those generated from humic organic matter, which is indicative of mixed source. With the ethane in Lower Paleozoic natural gases in the Ordos Basin become enriched in ^{13}C, the δD_{CH_4} shows unobvious change, which indicates that the origin of ethane is inconsistent with that of methane. Therefore, the geochemical parameters for ethane and other trace gases are used to identify the origins of natural gases dominated by methane may lead to an incorrect interpretation.

A significant difference exists in the distribution characteristics between natural gases generated from sapropelic organic matter and humic organic matter (Fig. 7). Natural gases generated from sapropelic organic matter have relatively less negative δD_{CH_4} and relatively negative $\delta^{13}C$ for ethane, while natural gases generated from humic organic matter have relatively negative δD_{CH_4} and relatively less negative $\delta^{13}C$ for ethane. The organic matter of the gas-source rocks in northwest Sichuan Basin, is type III but the sedimentary water medium is highly saline, which leads to deuterium enrichment in the methane. Natural gases in the Huanghua depression of Bohai Gulf Basin are generated principally from mixed type hydrocarbon source rocks and their sedimentary environment is

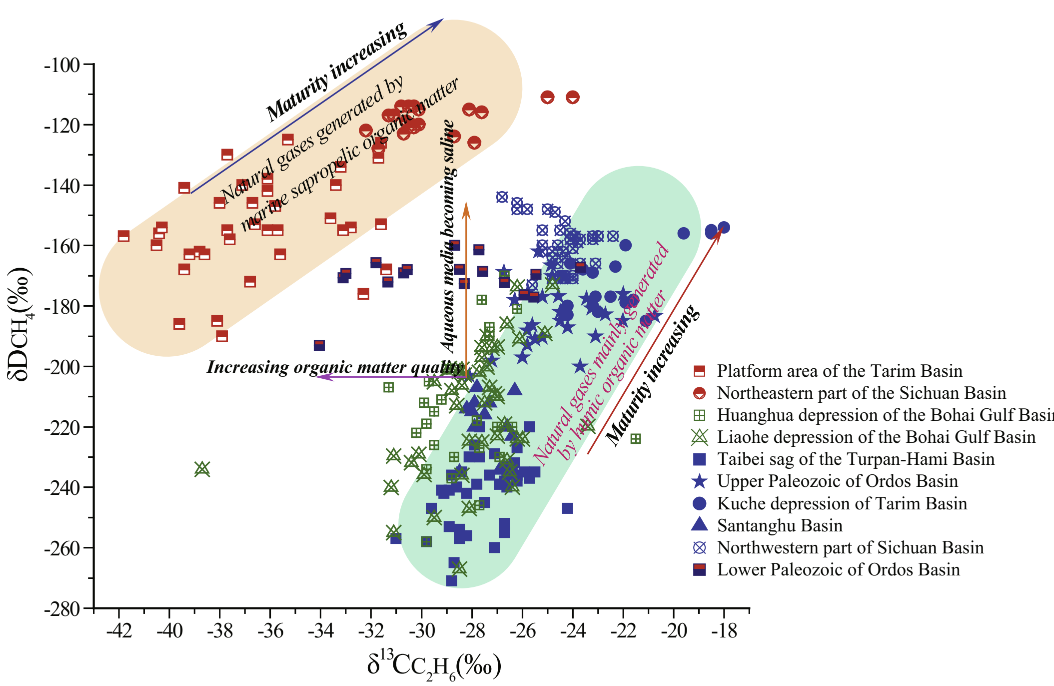

Fig. 7. Plot of δD_{CH_4} versus $\delta^{13}C_{C_2H_6}$ for thermogenic natural gases in Chinese sedimentary basins. The δD_{CH_4} and $\delta^{13}C_{C_2H_6}$ are related to the sedimentary environment of the hydrocarbon source which determines the type of organic matter and aqueous conditions. The $\delta^{13}C_{C_2H_6}$ shows more negative values when the organic matter type turns from type III to type I and methane shows more enrichment of D when the aqueous media becomes more saline. Therefore, natural gases generated from marine sapropelic organic matter occurs in the upper left of the figure and those mainly generated from humic organic matter occurs in the lower right.

brackish water. This leads to the $\delta^{13}C$ values of ethane in natural gases are less than –29‰ and the δD_{CH_4} values are slightly less negative than those in natural gases generated from typical freshwater swamp facies, coal series hydrocarbon source rocks (Fig. 7).

4. Conclusions

Three main factors influence δD_{CH_4} values in thermogenic natural gases from sedimentary basins of China. The first is the parent material, the δD of the organic matter in the hydrocarbon source rocks can influence the δD_{CH_4} value of the natural gas and the δD of the organic matter in the hydrocarbon source rocks reflect the sedimentary environment and the type of organic matter. Second, higher thermal maturity will result in D enrichment in the natural gases. A two-stage linear relationship exists between the δD_{CH_4} values and the log*R*o for natural gases generated from type III kerogen in sedimentary basins of China. Finally, the environmental conditions of the aqueous medium influence the δD_{CH_4} values in natural gases because elemental hydrogen from water participates in biochemical processes and exchanged during the sedimentation and diagenesis of organic matter, as well as during maturation of kerogen to generate gases. Among these factors, the aqueous medium is the key constraining factor and thermal maturity is the next.

Natural gases generated from sapropelic organic matter have relatively less negative δD_{CH_4} in sedimentary basins of China, while natural gases generated from humic organic matter have relatively negative δD_{CH_4}. Methane from the Xinchang gas field in northwestern Sichuan Basin is relatively enriched in D compared to other natural gases generated from type III kerogen because the aqueous media in which the hydrocarbon source rocks were deposited is quite saline. The δD_{CH_4} in Lower Paleozoic natural gases from the Ordos Basin show that these gases are derived from Carboniferous-Permian coal series and interfused with a minor amount of gas generated from Lower Paleozoic marine carbonate rocks. The δD_{CH_4} values in natural gases are geologically significant and a combination of δD and $\delta^{13}C$ values can be used to identify the origins of natural gases and to aid gas-source correlations.

Acknowledgements

This study was supported by National Basic Research Program of China (973 Program) Grant No. 2012CB214801 and the CAS Action-Plan for West Development, Grant No. KZCX2-XB3-12. We are grateful to associate editor, Dr. Maowen Li and two anonymous reviewers for their helpful comments and contributions that greatly improve the manuscript. We also gratefully acknowledge the time and effort contributed by Dr. John Volkman and Dr. Zhirong Zhang to improve the quality of paper.

Appendix A. Chemical and isotopic composition of natural gases from Chinese sedimentary basins

Basin	Sample	Formation	Depth(m)	Hydrogen isotopic composition(‰)			Carbon isotopic composition(‰)			Gas chemical composition (%)									Data source
				δD_{CH_4}	$\delta D_{C_2H_6}$	$\delta D_{C_3H_8}$	$\delta^{13}C_{CH_4}$	$\delta^{13}C_{C_2H_6}$	$\delta^{13}C_{C_3H_8}$	C_1	C_2	C_3	iC_4	nC_4	iC_5	nC_5	CO_2	N_2	
Taibei sag of the Turpan-Hami Basin	P10-6	J2q	n.d.	-236	-200	n.d.	-40.7	-27.3	-25.0	67.43	13.12	9.14	3.70	n.d.	n.d.	n.d.	0.11	6.31	This paper
	PB6	J2q	3547.8	-235	-195	-196	-39.9	-28.4	-26.1	68.28	11.32	7.45	2.17	2.05	0.61	0.51	0.41	6.71	
	P701	J2q	2256-2260	-240	-197	-194	-41.4	-28.6	-26.2	60.80	18.91	10.60	2.72	n.d.	n.d.	n.d.	0.43	6.34	
	P15-x	J2q	2432.4-2435.4	-236	-194	-198	-39.6	-28.8	-26.2	70.71	11.76	6.19	1.56	n.d.	n.d.	n.d.	0.24	9.39	
	Y17	K1s	1770-1797	-229	-189	-195	-39.6	-27.1	-25.4	53.83	17.80	12.40	3.63	n.d.	n.d.	n.d.	0.26	11.98	
	QD7	J2x	3107-3198	-257	-212	n.d.	-39.4	-28.5	-26.9	84.14	8.92	3.72	1.09	n.d.	n.d.	n.d.	0.10	1.95	
	QD9	J2x	3182-3217	-253	-209	n.d.	-40.5	-28.9	-27.0	84.95	8.65	3.28	0.91	n.d.	n.d.	n.d.	0.11	2.01	
	L7-20	J2s	2744-2785	-247	-221	-220	-42.2	-29.6	-27.2	75.53	11.88	7.02	2.32	n.d.	n.d.	n.d.	0.16	2.98	
	B27	J2x	1593-1900	-224	n.d.	n.d.	-39.8	n.d.	n.d.	n.d.	n.d.	n.d.	n.d.	n.d.	n.d.	n.d.	n.d.	n.d.	
	W8-35	J2s	2350-2409.5	-255	-217	-201	-39.3	-28.5	-26.4	82.99	8.93	3.98	1.41	n.d.	n.d.	n.d.	0.13	2.47	
	WS311	J2s	2626.17-2714	-241	-223	-223	-42.4	-29.2	-26.4	70.89	13.24	7.16	2.83	n.d.	n.d.	n.d.	0.65	5.13	
	L101	J2x	2707.5-2808.8	-258	n.d.	n.d.	-41.6	-29.8	-27.5	77.10	10.70	5.18	1.57	n.d.	n.d.	n.d.	2.84	2.32	
	HN901	K1s2	1854.0-1870.5	-230	-198	-214	-40.6	-28.1	-26.0	74.97	11.13	6.00	2.19	n.d.	n.d.	n.d.	0.26	5.26	
	HN901	J3k	1908-1928	-226	-197	-203	-42.0	-27.9	-25.8	63.93	17.51	9.92	3.41	n.d.	n.d.	n.d.	0.31	4.78	
	H801	J1s	4120-4140	-257	-224	-200	-43.1	-31.0	-28.7	61.52	14.53	11.16	4.18	n.d.	n.d.	n.d.	0.40	4.81	
	HT2-1	J2s	2321-2341	-242	-213	-166	-39.1	-28.2	-26.0	78.14	7.10	4.46	1.60	n.d.	n.d.	n.d.	1.04	7.52	
	HT2-10	J2s	2321-2341	-239	-207	n.d.	-37.6	-27.8	-25.8	83.66	7.79	3.61	1.01	n.d.	n.d.	n.d.	0.05	3.81	
	G1-1	J2s	3642.6-3589	-241	-203	-206	-41.2	-28.9	-26.5	68.47	12.40	7.88	2.47	n.d.	n.d.	n.d.	1.73	6.56	
	Mi2	J2x	3100-3105	-252	-223	-207	-40.4	-26.7	-26.0	80.97	8.71	4.57	1.48	1.13	0.55	0.36	0.11	1.50	
	QD26	J2x	3403-3450	-260	-223	-188	-41.8	-27.1	-26.4	44.16	14.38	16.06	7.65	6.54	3.95	2.54	0.11	0.08	
	L615	J2x	3030.4-3145.4	-256	-229	n.d.	-44.0	-28.2	-26.4	37.38	16.61	22.13	9.31	7.17	2.85	1.73	0.38	0.67	
	L3	J2s	2405.4-2420.4	-227	-200	-172	-41.5	-26.2	-23.8	n.d.	n.d.	n.d.	n.d.	n.d.	n.d.	n.d.	n.d.	n.d.	
	B18	J2x	1706-930	-247	-179	n.d.	-40.8	-24.2	-13.9	86.55	9.25	0.91	0.63	0.16	0.14	0.04	1.62	0.02	
	S8-151	J2x	3235.5-3266	-254	-230	-224	-43.3	-28.5	-27.4	56.15	11.36	13.54	6.77	5.04	2.33	1.47	0.07	1.57	
	S3-241	J2q	2933-2948	-245	-219	-207	-41.4	-27.5	-25.9	67.64	11.52	8.87	3.11	2.38	1.05	0.71	0.19	3.30	
	S13-15	J2s	3086	-220	-190	-161	-41.9	-27.7	-25.7	n.d.	n.d.	n.d.	n.d.	n.d.	n.d.	n.d.	n.d.	n.d.	
	W1	J2s	2341-2362	-240	-184	-114	-39.9	-26.6	-25.4	n.d.	n.d.	n.d.	n.d.	n.d.	n.d.	n.d.	n.d.	n.d.	
	WX1	J2s	2619.3-2627.1	-265	-249	-204	-43.0	-28.7	-24.7	80.75	8.42	3.53	0.91	0.74	0.34	0.30	0.11	3.29	
	WX1	J2x	2843-2860	-271	-249	-194	-43.4	-28.8	-24.7	n.d.	n.d.	n.d.	n.d.	n.d.	n.d.	n.d.	n.d.	n.d.	
	K7	J2x	1841.3-1848.3	-229	n.d.	n.d.	-41.7	n.d.	n.d.	n.d.	n.d.	n.d.	n.d.	n.d.	n.d.	n.d.	n.d.	n.d.	
	TC1	J2s	2808-3247.4	-242	n.d.	n.d.	-44.8	-29.1	-22.1	n.d.	n.d.	n.d.	n.d.	n.d.	n.d.	n.d.	n.d.	n.d.	
	WX8	J2q	2830-2817	-255	-220	-213	-39.3	-26.7	-25.6	n.d.	n.d.	n.d.	n.d.	n.d.	n.d.	n.d.	n.d.	n.d.	
	L10	Esh	663-706	-230	-210	n.d.	-43.1	-27.7	-22.6	78.69	10.04	4.86	1.34	1.01	0.42	0.26	2.08	0.82	
	SN2-1	J2s	n.d.	-232	-200	-186	-39.1	-26.3	-24.9	56.23	11.08	13.15	5.97	5.85	1.90	1.02	0.10	3.97	
	PB103	J2s	3484.5-3520.1	-239	-200	-175	-40.2	-26.9	-25.3	6.44	0.26	0.08	0.02	0.01	0.01	n.d.	0.22	92.95	
	P6-1	J2q	2406.5-2409.5	-235	-194	-174	-39.2	-25.5	-24.3	62.85	7.49	9.05	3.55	3.15	0.98	0.70	0.21	11.34	
	S118	K	2031.3-2051.2	-233	-197	-182	-39.0	-26.6	-25.1	65.24	15.07	9.43	2.35	2.09	0.57	0.35	0.13	4.50	
	S110	Esh	1898-1902.6	-238	-192	-183	-39.4	-26.2	-24.7	10.71	19.97	35.40	12.78	11.86	3.62	2.52	0.04	0.66	
	S233	J2s	2434.7-2629.6	-234	-198	-192	-38.7	-26.4	-24.9	n.d.	n.d.	n.d.	n.d.	n.d.	n.d.	n.d.	n.d.	n.d.	
	SN8	J2q	2624-2634	-239	-192	-167	-39.6	-26.9	-25.2	38.68	25.98	20.69	5.54	4.86	0.83	0.46	0.11	2.57	
	G1	J2s	3576-3589	-236	-201	-184	-40.0	-26.6	-25.2	78.89	9.86	4.54	0.95	0.72	0.19	0.13	0.18	4.39	
	SB402	K	1784.6-1792	-220	-189	-174	-39.0	-25.7	-23.6	66.69	14.51	9.49	2.01	1.86	0.48	0.36	0.02	3.51	
	L12	K	1627.6-1637.6	-236	-201	-184	-42.6	-26.2	-24.5	n.d.	n.d.	n.d.	n.d.	n.d.	n.d.	n.d.	n.d.	n.d.	
	LN1	J3k	2009-2017	-238	-203	-176	-41.7	-26.7	-25.1	79.84	8.92	5.08	1.33	1.13	0.38	0.27	n.d.	2.84	
	HT202	J3q	1687.6-1700	-235	-205	-199	-37.2	-25.9	-24.8	80.27	7.44	3.96	1.18	1.08	0.42	0.29	0.56	4.24	
	HT204	J2s	2306.2-2322.8	-237	-205	-199	-36.9	-25.7	-24.4	83.02	7.90	3.69	1.00	0.94	0.35	0.24	0.09	2.42	

Basin		Sample	Formation	Depth(m)	Hydrogen isotopic composition(‰)			Carbon isotopic composition(‰)			Gas chemical composition (%)									Data source
					δD_{CH_4}	$\delta D_{C_2H_6}$	$\delta D_{C_3H_8}$	$\delta^{13}C_{CH_4}$	$\delta^{13}C_{C_2H_6}$	$\delta^{13}C_{C_3H_8}$	C_1	C_2	C_3	iC_4	nC_4	iC_5	nC_5	CO_2	N_2	
Ordos Basin	Upper Paleozoic	S33-18	n.d.	n.d.	-185	-164	n.d.	-34.9	-24.5	-25.9	72.72	3.11	0.50	0.07	0.12	0.04	0.02	0.75	16.94	This paper
		S35-17	n.d.	3313	-187	-159	-158	-35.1	-24.2	-25.2	90.44	4.60	0.79	0.11	0.15	0.05	0.03	1.14	1.94	
		S38-14	n.d.	3322-3373	-190	-169	-227	-35.6	-25.2	-25.3	89.33	5.87	1.23	0.19	0.21	0.07	0.04	1.03	1.18	
		S38-16	n.d.	3313.5	-188	-164	-204	-35.6	-25.8	-25.5	89.96	4.64	0.96	0.16	0.17	0.06	0.03	2.01	1.27	
		S22-15	n.d.	3304	-182	-164	n.d.	-32.5	-24.5	-26.4	82.66	3.12	0.72	0.12	0.15	0.05	0.03	1.03	5.04	
		S13-16	n.d.	n.d.	-186	-156	n.d.	-32.6	-25.6	-23.5	89.90	4.67	0.87	0.14	0.15	0.06	0.03	1.43	1.92	
		Shan215	C-P	n.d.	-193	-167	-155	-30.0	-25.8	-24.2	93.60	3.79	0.55	0.08	0.08	0.08	n.d.	0.76	0.86	Cai et al.,2005
		Shan117	C-P	n.d.	-197	-163	-156	-32.2	-26.0	-24.9	92.60	3.99	0.63	0.10	0.11	0.15	n.d.	1.51	0.71	
		Zhao4	C-P	n.d.	-200	-164	-163	-31.3	-23.7	-23.0	90.70	5.46	1.09	0.21	0.21	0.25	n.d.	0.45	1.35	
		Qi2	C-P	n.d.	-177	-163	-156	-31.6	-25.2	-22.8	91.30	3.02	0.46	0.07	0.07	0.09	n.d.	2.67	1.90	
		Yu17-2	C-P	n.d.	-191	-157	-147	-34.2	-25.5	-23.1	91.20	5.31	0.84	0.14	0.14	0.15	n.d.	n.d.	n.d.	
		Yu12	C-P	n.d.	-178	-148	-140	-34.2	-26.3	-24.0	91.20	5.81	0.84	0.17	0.16	0.24	n.d.	n.d.	n.d.	
		Mi4	C-P	n.d.	-176	-155	-160	-28.1	-22.0	-22.7	n.d.	n.d.	n.d.	n.d.	n.d.	n.d.	n.d.	n.d.	n.d.	Feng et al., 2007
		Meng5	n.d.	n.d.	-214	-158	-158	-36.2	-28.1	-24.8	n.d.	n.d.	n.d.	n.d.	n.d.	n.d.	n.d.	n.d.	n.d.	
		Su33-18	n.d.	n.d.	-190	-173	-181	-31.7	-23.1	-23.4	n.d.	n.d.	n.d.	n.d.	n.d.	n.d.	n.d.	n.d.	n.d.	
		Su40-16	n.d.	n.d.	-198	-162	-173	-30.2	-27.2	-25.5	n.d.	n.d.	n.d.	n.d.	n.d.	n.d.	n.d.	n.d.	n.d.	
		Yu17-1	n.d.	n.d.	-203	-150	-135	-36.7	-28.1	-23.2	n.d.	n.d.	n.d.	n.d.	n.d.	n.d.	n.d.	n.d.	n.d.	
		Shan10	P1x	n.d.	-169	n.d.	n.d.	-31.0	-26.7	-28.6	85.26	2.83	0.27	0.02	0.04	n.d.	n.d.	1.05	10.47	Li et al., 2008
		Shan19	P1x	n.d.	-167	n.d.	n.d.	-35.1	-24.8	-24.5	94.91	1.41	0.14	0.02	0.02	0.01	n.d.	1.29	1.90	
		Shan65	P1x	n.d.	-178	n.d.	n.d.	-29.1	-23.4	-25.4	95.74	2.54	0.29	0.03	0.04	0.03	n.d.	0.13	1.10	
		Shan16	P1s	n.d.	-162	n.d.	n.d.	-31.3	-25.3	-25.8	85.84	0.99	0.11	0.01	0.01	n.d.	n.d.	0.90	10.86	
		Shan 3	P1s	n.d.	-170	n.d.	n.d.	-33.6	-24.8	-26.0	95.24	1.36	0.27	0.11	0.17	n.d.	n.d.	0.07	1.46	
		Shan 41	P1s	n.d.	-177	n.d.	n.d.	-33.4	-24.6	-25.0	95.02	3.06	0.45	0.05	0.05	n.d.	n.d.	n.d.	1.15	
		Shan 46	P1s	n.d.	-183	n.d.	n.d.	-31.0	-22.7	-21.3	85.80	7.67	2.07	0.49	0.38	n.d.	n.d.	1.20	1.33	
		Shan 56	P1s	n.d.	-185	n.d.	n.d.	-33.3	-22.0	-20.7	85.04	6.03	1.56	0.52	0.35	n.d.	n.d.	n.d.	3.20	
		Shan 68	P1s	n.d.	-172	n.d.	n.d.	-34.8	-29.3	-27.8	90.97	5.91	1.11	0.25	0.16	n.d.	n.d.	4.06	0.90	
		Shan 83	P1s	n.d.	-183	n.d.	n.d.	-32.6	-20.8	-19.6	93.32	3.39	0.45	0.17	0.07	n.d.	n.d.	0.80	15.70	
		Shan 26	C3t	n.d.	-181	n.d.	n.d.	-33.5	-23.2	-23.0	87.22	1.84	0.17	0.02	0.02	n.d.	n.d.	7.05	3.03	
		Shan 19	C2b	n.d.	-175	n.d.	n.d.	-35.4	-25.8	-24.9	94.95	1.86	0.24	0.04	0.03	n.d.	n.d.	2.69	0.12	
	Lower Paleozoic	Shan 5	O1m5	n.d.	-172	n.d.	n.d.	-33.8	-31.3	-27.1	97.25	0.49	0.06	0.01	0.01	n.d.	n.d.	1.65	0.33	
		Shancan1	O1m5	n.d.	-169	n.d.	n.d.	-33.9	-27.6	-26.0	93.33	0.67	0.08	0.01	0.01	n.d.	n.d.	2.71	3.19	
		Shan 12	O1m5	n.d.	-170	n.d.	n.d.	-34.2	-25.5	-26.4	96.79	0.78	0.10	0.01	0.01	n.d.	n.d.	1.65	0.63	
		Shan 17	O1m5	n.d.	-169	n.d.	n.d.	-33.2	-30.7	-26.9	93.87	0.72	0.08	0.01	0.01	n.d.	n.d.	4.55	0.62	
		Shan 6	O1m5	n.d.	-193	n.d.	n.d.	-33.9	-34.1	-24.4	92.60	0.32	0.03	n.d.	n.d.	n.d.	n.d.	4.86	2.22	
		Lin 2	O1m5	n.d.	-176	n.d.	n.d.	-35.2	-25.9	-25.4	95.34	1.40	0.18	0.02	0.03	n.d.	n.d.	2.62	0.39	
		Shan 33	O1m5	n.d.	-172	n.d.	n.d.	-34.0	-26.7	-25.5	98.87	0.98	0.11	0.02	0.01	n.d.	n.d.	n.d.	n.d.	
		Shan 34	O1m5	n.d.	-177	n.d.	n.d.	-35.3	-25.5	-24.4	94.02	1.28	0.15	0.04	0.02	n.d.	n.d.	0.36	4.11	
		Shan 45	O1m5	n.d.	-168	n.d.	n.d.	-33.5	-30.6	-22.9	94.92	0.16	0.04	n.d.	n.d.	n.d.	n.d.	4.44	0.25	
		Shan 49	O1m5	n.d.	-166	n.d.	n.d.	-33.4	-31.8	n.d.	94.64	0.31	0.03	n.d.	n.d.	n.d.	n.d.	4.52	0.47	
		Shan 61	O1m5	n.d.	-162	n.d.	n.d.	-34.0	-27.7	-28.4	97.50	0.77	0.10	0.01	0.01	n.d.	n.d.	1.61	n.d.	
		Shan 81	O1m5	n.d.	-160	n.d.	n.d.	-30.9	-28.7	-25.1	93.24	0.81	0.13	0.02	0.02	n.d.	n.d.	2.57	3.19	
		Shan 84	O1m5	n.d.	-168	n.d.	n.d.	-31.8	-28.5	-24.2	92.40	0.81	0.12	0.01	0.01	n.d.	n.d.	5.09	0.99	
		Shan 62	O1m5	n.d.	-171	n.d.	n.d.	-32.7	-33.1	-30.0	96.55	0.54	0.07	0.01	0.01	n.d.	n.d.	2.15	0.64	
		Shan 30	O1m5	n.d.	-169	n.d.	n.d.	-32.8	-33.0	-25.0	95.23	0.43	0.05	n.d.	n.d.	n.d.	n.d.	2.81	1.44	
		Shan 28	O1m5	n.d.	-173	n.d.	n.d.	-34.1	-28.3	-27.3	95.96	0.74	0.09	0.01	0.01	n.d.	n.d.	2.84	0.25	
		Shan 7	O1m5	n.d.	-167	n.d.	n.d.	-36.2	-23.7	-23.5	93.67	1.28	0.17	0.03	0.03	n.d.	n.d.	4.67	0.15	
Tarim Basin	Kuche Depression	YH701	E	5160-5168	-180	-134	-131	-34.8	-24.2	-21.6	82.57	8.79	2.62	0.50	0.67	0.18	0.20	0.63	3.19	This paper
		YH2	N	4953-4957	-181	-133	-134	-34.4	-24.3	-21.8	81.59	9.21	2.72	0.50	0.63	0.16	0.16	1.44	3.17	
		YH1	E	5451-5466	-179	-113	-126	-33.4	-21.9	-17.5	84.53	7.58	0.89	0.36	0.51	0.18	0.26	0.12	3.75	
		DN22	E	4748-4774	-177	-126	-147	-35.1	-22.5	-20.5	88.18	7.06	1.49	0.31	0.34	0.12	0.11	0.50	0.99	
		DN201	E	4980-4990	-177	-125	-142	-35.2	-23.1	-19.7	87.53	7.57	1.60	0.31	0.34	0.11	0.10	0.65	0.96	
		YH23-2-10	E+K	5134-5189	-183	-134	-145	-34.4	-24.2	-21.5	82.16	8.86	2.61	0.48	0.59	0.15	0.15	0.71	3.34	
		YH23-1-5	N	4946-4957	-185	-139	-123	-30.7	-21.1	-19.2	82.95	8.72	1.55	0.44	0.60	0.18	0.21	0.46	3.94	
		DW105-25	N	367-395	-156	n.d.	n.d.	-28.5	-19.6	-13.2	89.29	3.40	0.39	0.13	0.17	0.07	0.08	n.d.	1.25	
		YTK5	E	5310-5315	-169	n.d.	n.d.	-33.4	-23.2	-23.5	83.97	7.35	1.24	0.49	0.74	0.23	0.23	n.d.	5.05	
		DN202	K	5192-5280	-182	n.d.	n.d.	-34.4	-23.0	-20.1	87.70	7.46	1.55	0.31	0.34	0.12	0.11	0.45	0.96	
		KL2-4	E	n.d.	-163	n.d.	n.d.	-27.4	-17.5	-20.1	97.56	0.52	0.07	n.d.	0.02	n.d.	n.d.	0.57	1.13	
		KL2-7	E	n.d.	-163	n.d.	n.d.	-27.3	-17.7	-21.1	97.94	0.52	0.06	n.d.	0.02	n.d.	n.d.	0.64	0.79	
		KL2-8	E	n.d.	-164	n.d.	n.d.	-27.3	-18.1	-20.0	97.61	0.52	0.07	n.d.	0.02	n.d.	n.d.	0.64	1.04	
		KL205	E	n.d.	-162	n.d.	n.d.	-27.0	-18.3	-25.1	97.34	0.53	0.08	n.d.	0.02	n.d.	n.d.	0.66	1.19	
		YH701	E	6000	-180	-137	-104	-32.8	-23.3	-21.0	82.60	5.66	2.24	n.d.	1.68	n.d.	n.d.	0.22	4.00	Lui et al., 2008
		YH23-1-18	E+K	n.d.	-181	-135	-106	-31.7	-23.0	-20.6	86.46	5.80	2.17	n.d.	1.37	n.d.	n.d.	0.47	3.74	
		YH23-1-14	E+K	n.d.	-180	-132	-103	-32.3	-23.2	-20.4	85.89	6.23	2.24	n.d.	1.61	n.d.	n.d.	0.26	3.77	
		YH1	K	5600	-179	-135	-106	-30.9	-21.8	-22.3	77.65	7.91	2.92	n.d.	2.61	n.d.	n.d.	1.59	3.16	
		YTK5-3	E+K	n.d.	-168	-126	-104	-34.7	-23.6	-21.6	85.97	6.91	2.76	n.d.	1.75	n.d.	n.d.	0.32	2.29	
		YTK5-2	E	n.d.	-166	-130	-106	-34.2	-24.1	-22.8	83.10	6.94	3.67	n.d.	3.08	n.d.	n.d.	0.14	3.09	
		KL2-8	E	n.d.	-156	-119	-100	-27.3	-18.5	-19.5	97.96	0.82	0.05	n.d.	0.02	n.d.	n.d.	0.54	0.62	
		KL2-7	E	n.d.	-154	-118	-100	-27.6	-18.0	-19.9	98.41	0.80	0.05	n.d.	0.02	n.d.	n.d.	0.05	0.69	
		KL203	E	4050	-155	-117	-97	-27.3	-18.5	-19.0	97.86	0.82	0.05	n.d.	0.03	n.d.	n.d.	0.66	0.58	
		HQ1	n.d.	n.d.	-167	-112	-104	-32.4	-22.3	-21.4	55.95	11.55	12.53	n.d.	7.22	n.d.	n.d.	0.20	4.96	
		HQ2	n.d.	5540	-167	-112	-104	-32.4	-22.3	-21.4	55.95	11.55	12.53	n.d.	7.22	n.d.	n.d.	0.20	4.96	
		DW117-3	N	285-518	-178	-122	-85	-32.8	-21.6	-21.2	88.31	4.72	1.53	n.d.	0.91	n.d.	n.d.	n.d.	4.53	
		DN102	N	5768.11	-179	-120	-110	-33.5	-21.1	-19.7	74.24	10.46	4.90	n.d.	1.84	n.d.	n.d.	1.50	5.58	
		QL1	K	5930	-163	-130	-111	-31.2	-23.9	-22.8	84.38	6.80	3.23	n.d.	2.92	n.d.	n.d.	0.17	2.50	
		TRG1	E	4836.5-4839.5	-189	-134	-107	-35.4	-22.7	-20.9	85.36	7.03	2.98	n.d.	2.25	n.d.	n.d.	0.28	2.10	
		TRG101	K	5298	-191	-133	-111	-32.8	-23.4	-21.1	86.65	6.31	2.74	n.d.	1.76	n.d.	n.d.	0.31	2.22	
		YM7-H1	E	n.d.	-160	-112	-75	-32.4	-22.7	-19.8	90.14	4.62	1.27	n.d.	1.25	n.d.	n.d.	0.12	2.58	
		DW109-19	N	456-461	-160	-123	-81	-29.7	-21.9	-21.2	90.04	5.49	1.50	n.d.	0.95	n.d.	n.d.	n.d.	2.01	
	Platform Area	DH20	n.d.	n.d.	-168	-122	-101	-40.5	-31.4	-29.8	79.30	9.36	3.27	n.d.	1.83	n.d.	n.d.	0.41	4.89	
		DH23	P	5700	-176	-128	-109	-40.0	-32.3	-30.3	82.92	6.52	2.65	n.d.	0.68	n.d.	n.d.	2.38	4.29	
		JLK102	T	4336-4342	-141	-136	-113	-34.9	-39.4	-32.0	87.03	3.18	1.45	n.d.	1.36	n.d.	n.d.	0.16	6.83	
		JFQ1-13-4	T	n.d.	-155	-155	-130	-35.4	-36.1	-33.8	73.63	3.71	1.98	n.d.	0.79	n.d.	n.d.	1.02	18.04	
		JN4-H2	T	n.d.	-142	-137	-117	-35.8	-36.1	-33.2	80.94	3.86	2.46	n.d.	1.20	n.d.	n.d.	1.34	8.62	
		TZ117	S	4510	-162	-129	-119	-40.0	-38.8	-33.2	69.68	6.16	3.75	n.d.	2.22	n.d.	n.d.	0.57	14.35	
		TZ16-6	O	n.d.	-160	-173	-149	-41.2	-40.5	-33.0	41.00	5.16	8.64	n.d.	9.07	n.d.	n.d.	3.56	25.97	
		TZ242	O	n.d.	-125	-145	-130	-37.1	-35.3	-32.1	89.88	1.64	0.56	n.d.	0.35	n.d.	n.d.	1.84	5.59	
		TZ4-18-7	C	n.d.	-156	-164	-131	-42.6	-40.4	-33.6	72.42	5.03	2.38	n.d.	0.86	n.d.	n.d.	0.74	17.47	
		TZ62	C	4758	-126	-121	-115	-37.1	-31.6	-30.1	90.03	1.52	0.68	n.d.	0.46	n.d.	n.d.	2.76	4.41	
		TZ621	O	4885	-131	-135	-120	-36.6	-31.7	-29.2	87.31	1.87	1.11	n.d.	1.17	n.d.	n.d.	1.91	4.16	
		LN59-H1	C	n.d.	-130	-124	-95	-38.9	-37.7	-34.6	94.45	1.14	0.20	n.d.	0.21	n.d.	n.d.	3.66	0.34	
		LG13	O	5685	-134	-128	-100	-33.8	-33.2	-29.2	95.12	1.50	0.33	n.d.	0.31	n.d.	n.d.	1.60	1.14	
		LG201	O	5400	-140	-160	-142	-35.6	-37.1	-34.0	86.06	2.21	1.26	n.d.	0.71	n.d.	n.d.	4.86	4.09	

Basin		Sample	Formation	Depth(m)	Hydrogen isotopic composition(‰)			Carbon isotopic composition(‰)			Gas chemical composition（%）									Data source
					δD_{CH_4}	$\delta D_{C_2H_6}$	$\delta D_{C_3H_8}$	$\delta^{13}C_{CH_4}$	$\delta^{13}C_{C_2H_6}$	$\delta^{13}C_{C_3H_8}$	C_1	C_2	C_3	iC_4	nC_4	iC_5	nC_5	CO_2	N_2	
		LG16-2	O	n.d.	-138	-143	-121	-34.3	-36.1	-33.4	92.80	2.05	0.89	n.d.	0.38	n.d.	n.d.	1.64	1.71	
		LG15-18	O	n.d.	-190	-191	-142	-41.3	-37.9	-34.5	61.96	7.37	6.12	n.d.	4.08	n.d.	n.d.	7.14	7.12	
		LN2-33-1	T	n.d.	-147	-154	-123	-32.0	-35.8	-31.9	81.83	3.48	2.25	n.d.	1.22	n.d.	n.d.	0.64	8.47	
		TZ16-13	S	4009.5-4057	-157	-217	-208	-41.1	-41.8	-38.5	n.d.	n.d.	n.d.	n.d.	n.d.	n.d.	n.d.	n.d.	n.d.	This paper
		TZ4-37-H18	C	3590.66	-163	n.d.	n.d.	-45.4	-39.2	-26.4	67.93	3.70	1.12	0.46	0.96	0.30	0.49	0.25	22.61	
		TZ4-401-H2	C	3724	-163	n.d.	n.d.	-42.7	-38.6	-35.3	74.79	2.86	0.64	0.14	0.25	0.05	0.07		20.33	
		TZ4-7-24	C	3608-3626	-154	n.d.	n.d.	-42.7	-40.3	-32.6	74.86	3.49	1.11	0.38	0.79	0.14	0.20	1.18	17.11	
		LK1	n.d.	n.d.	-168	-181	-168	-40.2	-39.4	-33.3	n.d.	n.d.	n.d.	n.d.	n.d.	n.d.	n.d.	n.d.	n.d.	
		YN2c	J	3613.5-3705.03	-151	-122	-102	-35.9	-33.6	-28.4	n.d.	n.d.	n.d.	n.d.	n.d.	n.d.	n.d.	n.d.	n.d.	
		YN2	S	3534-3555	-154	-105	-84	-35.6	-32.8	-27.9	76.76	5.99	1.84	n.d.	0.95	n.d.	n.d.	0.13	13.83	
		LN3-H1	n.d.	4870-5314	-172	-181	-141	-37.3	-36.8	-34.5	71.74	2.15	0.62	0.15	0.24	0.07	0.09		16.52	
		LN3-H5	n.d.	5182.55-5383.0	-153	-187	-155	-35.3	-36.6	-37.4	84.65	2.92	0.89	0.32	0.70	0.24	0.37	0.06	8.52	
		JF132	n.d.	4419.5-4422	-155	-145	-148	-36.6	-35.7	-33.0	n.d.	n.d.	n.d.	n.d.	n.d.	n.d.	n.d.	n.d.	n.d.	
		LG17	n.d.	5400-5468	-140	n.d.	n.d.	-35.4	-33.4	-31.5	n.d.	n.d.	n.d.	n.d.	n.d.	n.d.	n.d.	n.d.	n.d.	
		LN15-2	n.d.	n.d.	-186	n.d.	n.d.	-41.4	-39.6	-36.0	n.d.	n.d.	n.d.	n.d.	n.d.	n.d.	n.d.	n.d.	n.d.	
		LN10-2	n.d.	n.d.	-163	-152	n.d.	-37.1	-35.6	-32.2	77.67	4.47	1.10	0.36	0.67	0.21	0.31	3.88	10.37	
		JFQ132	T	4419.5-4422	-155	-145	-148	-36.3	-33.1	-32.3	88.12	2.01	1.61	n.d.	2.49	n.d.	n.d.	0.18	6.05	
		JFQ138	T	4556-4563	-153	-157	-132	-35.3	-31.6	-28.6	73.18	3.56	1.05	n.d.	1.19	n.d.	n.d.	1.05	18.68	
		LN204	n.d.	4867-4871	-146	-183	-153	-35.4	-38.0	-34.4	n.d.	n.d.	n.d.	n.d.	n.d.	n.d.	n.d.	n.d.	n.d.	
		LN2-25-H1	n.d.	4944.0-5260.3	-146	-180	-154	-34.1	-36.7	-32.5	90.55	1.71	0.57	0.13	0.24	0.05	0.07	0.88	4.94	
		HD1-1H	n.d.	5112.7-5448.62	-185	-154	-130	-41.6	-38.1	-33.8	58.86	4.89	1.29	0.33	0.55	0.09	0.11		32.27	
		MA4	O	n.d.	-155	n.d.	n.d.	-37.6	-37.7	-33.7	84.90	1.51	0.58	n.d.	0.27	n.d.	n.d.	1.53	10.85	
		MA4-H1	O	n.d.	-158	n.d.	n.d.	-38.0	-37.6	-32.7	83.88	1.55	0.67	n.d.	0.32	n.d.	n.d.	0.09	13.08	
Sichuan Basin	Northeastern part of Sichuan Basin	PG7	T_1f^1	5571.7-5590	-114	n.d.	n.d.	-30.8	-30.8	n.d.	76.66	0.41	0.01	n.d.	n.d.	n.d.	n.d.	8.45	0.57	This paper
		PG7	T_1f^2	5484.7-5546.7	-115	n.d.	n.d.	-31.1	-30.1	n.d.	77.66	0.38	0.01	n.d.	n.d.	n.d.	n.d.	8.52	0.60	
		PG7C1	T_1f^2	5421.4-5464.2	-120	n.d.	n.d.	-30.7	-30.1	n.d.	78.83	0.03	n.d.	n.d.	n.d.	n.d.	n.d.	9.83	0.30	
		PG8	P_{2ch}	5614-5625.5	-119	n.d.	n.d.	-30.9	-30.6	n.d.	82.12	0.02	n.d.	n.d.	n.d.	n.d.	n.d.	9.48	1.44	
		PG9	T_1f^3	5739.0-5852.3	-115	n.d.	n.d.	-30.9	-28.1	n.d.	76.28	0.41	0.02	n.d.	n.d.	n.d.	n.d.	8.66	0.50	
		PG9	T1f3-T1f1	5915.8-5993	-114	n.d.	n.d.	-31.1	-30.5	n.d.	77.06	0.02	n.d.	n.d.	n.d.	n.d.	n.d.	8.30	0.90	
		PG9	P_2ch	6110.0-6130.0	-124	n.d.	n.d.	-30.9	-28.7	n.d.	72.96	0.03	n.d.	n.d.	n.d.	n.d.	n.d.	11.54	1.05	
		PG9	P_2ch	6151.0-6175.0	-122	n.d.	n.d.	-30.9	-32.2	n.d.	72.67	0.03	n.d.	n.d.	n.d.	n.d.	n.d.	11.18	1.12	
		PG101	T_1f^2	5775.7-5786.4	-114	n.d.	n.d.	-27.8	-30.3	n.d.	76.24	0.41	0.02	n.d.	n.d.	n.d.	n.d.	8.45	0.38	
		DW1	T1f3-T1f2	5029.0-5130.0	-120	n.d.	n.d.	-32.5	-30.4	n.d.	73.42	0.45	0.02	n.d.	n.d.	n.d.	n.d.	8.86	1.24	
		DW1	T_1f^1	5153.0-5279.0	-117	n.d.	n.d.	-30.0	-31.3	n.d.	50.01	0.40	0.33	n.d.	0.04	n.d.	n.d.	32.26	3.36	
		DW1	P_2ch	5320.0-5382	-111	n.d.	n.d.	-31.3	-24.0	n.d.	66.68	0.41	0.06	n.d.	0.01	n.d.	n.d.	11.70	3.21	
		DW2	T_1f	4804.4-4900.0	-123	n.d.	n.d.	-28.9	-30.7	n.d.	74.95	0.03	n.d.	n.d.	n.d.	n.d.	n.d.	10.04	0.89	
		QX1	T1f4-T1f3	4285	-128	n.d.	n.d.	-27.0	-31.7	n.d.	98.52	0.30	n.d.	n.d.	n.d.	n.d.	n.d.	0.03	1.01	
		MB4	T_1f^1	4049.6-4102.0	-117	n.d.	n.d.	-31.2	-31.1	n.d.	67.31	0.37	0.01	n.d.	n.d.	n.d.	n.d.	16.31	3.15	
		MB6	T1f2-T1f1	3857.8-3970.0	-126	n.d.	n.d.	-31.9	-27.9	n.d.	73.85	0.41	0.01	n.d.	n.d.	n.d.	n.d.	7.67	1.28	
		MB6	T_1f^3	4744.9-4841.0	-121	n.d.	n.d.	-32.1	-30.3	n.d.	75.17	0.43	0.01	n.d.	n.d.	n.d.	n.d.	8.45	0.87	
		YB1	T_1f^3	6787.0-6799.0	-111	n.d.	n.d.	-28.7	-25.0	n.d.	75.65	0.07	0.03	n.d.	n.d.	n.d.	n.d.	14.05	9.27	
		YB1	P_2ch	7081.0-7150.0	-116	n.d.	n.d.	-30.2	-27.6	n.d.	50.06	0.40	0.34	n.d.	0.04	n.d.	n.d.	32.10	3.11	
	Northwestern part of Sichuan Basin	Zhong 19	T3x2	2602	-170	-144	-135	-35.0	-24.0	-22.5	90.36	5.81	1.53	0.31	0.36	0.12	0.09	0.45	0.63	Dai et al., 2012b
		Zhong 34	T3x2	2408	-170	-143	-135	-35.4	-24.5	-22.8	90.80	5.70	1.43	0.30	0.34	0.11	0.08	0.48	0.53	
		Zhong 36	T3x2	2628	-171	-143	-136	-35.4	-24.4	-22.9	90.90	5.75	1.49	0.31	0.35	0.11	0.08	0.52	0.21	
		Zhong 44	T3x2	2510	-171	-145	-137	-35.0	-24.0	-22.7	90.19	5.79	1.55	0.32	0.36	0.11	0.08	0.47	0.91	
		Zhong 63	T3x2	2366	-170	-145	-136	-35.5	-24.4	-23.0	91.00	5.75	1.43	0.31	0.35	0.11	0.08	0.46	0.28	
		Zhong 2	T3x2	2578.5	-171	-146	-137	-35.3	-24.3	-23.0	90.53	5.75	1.46	0.32	0.36	0.13	0.09	0.54	0.46	
		Zhong 16	T3x2	2446	-171	-147	-138	-35.6	-24.3	-22.8	89.80	6.10	1.65	0.38	0.43	0.14	0.11	0.56	0.49	
		Zhong 2	T3x2	2400	-170	-144	-136	-35.5	-24.3	-22.9	90.82	5.77	1.44	0.31	0.36	0.12	0.09	0.47	0.27	
		Zhong 29	T3x2	2269-2361	-171	-133	n.d.	-34.8	-24.8	-23.7	87.86	6.53	2.10	0.60	0.83	n.d.	n.d.	0.39	0.28	
		Zhong 39	T3x2	2422.9	-173	-147	n.d.	-36.9	-25.6	-23.2	87.82	6.36	2.70	0.93	1.39	n.d.	n.d.	0.32	0.03	
		QX 006-X 1	T3x2	3605.1	-157	-132	-139	-31.6	-22.4	-22.4	93.17	4.12	0.71	0.13	0.11	0.02	0.01	1.36	0.26	
		QX 6	T3x2	3360	-158	-132	-118	-31.2	-23.2	-23.1	95.95	2.48	0.30	0.04	0.04	0.01	n.d.	0.92	0.21	
		QX 16	T3x2	3374.2	-159	-134	-139	-30.8	-23.8	n.d.	96.46	1.74	0.16	0.02	0.02	n.d.	n.d.	1.39	0.20	
		QX 4	T3x2	3682	-157	-133	-137	-32.9	-23.2	-23.0	93.52	3.91	0.62	0.10	0.08	0.01	0.01	1.47	0.24	
		QX 13	T3x2	3934.5	-158	-134	-137	-33.7	-24.1	-23.4	93.49	3.90	0.63	0.11	0.08	0.02	0.01	1.47	0.25	
		QX 3	T3x2	3524.5	-157	-133	-135	-33.1	-23.0	-22.7	93.30	3.91	0.63	0.10	0.08	0.01	0.01	1.67	0.25	
		Xin 882	T3x4	3383.6-3405.6	-166	-139	-132	-34.3	-23.1	-21.4	n.d.	n.d.	n.d.	n.d.	n.d.	n.d.	n.d.	n.d.	n.d.	
		XQ 105	J	n.d.	-162	-135	-122	-33.4	-24.4	-22.1	85.38	4.87	1.25	0.21	0.26	0.05	0.03	n.d.	7.93	
		CX 480-1	J	n.d.	-166	-135	-102	-34.8	-23.7	-20.1	91.65	5.70	1.34	0.27	0.30	0.07	0.05	n.d.	0.32	
		CX 480-2	J	n.d.	-162	-135	-132	-34.6	-24.4	-22.1	92.62	4.94	1.23	0.26	0.26	0.07	0.04	n.d.	0.32	
		CX 263	J	n.d.	-162	-131	-122	-33.4	-24.8	-22.3	91.95	5.20	1.46	0.26	0.35	0.08	0.06	n.d.	0.36	
		JS 12	J	1658-1670	-162	-135	-110	-34.4	-25.2	-22.3	88.82	5.66	1.95	0.42	0.51	0.13	0.10	n.d.	2.01	
		JS 17	J	1524-1557	-164	-133	-117	-34.7	-24.8	-22.1	89.60	5.66	1.89	0.41	0.49	0.13	0.10	n.d.	1.20	
		Long 3	J	980	-157	-131	-128	-34.0	-23.0	-21.0	86.41	5.00	1.76	0.39	0.51	0.12	0.10	n.d.	5.33	
		LS 35	J	1489	-161	-133	-102	-33.5	-24.0	-21.5	88.72	6.00	2.03	0.41	0.52	0.12	0.10	n.d.	1.70	
		Long 45-1	J	610	-157	-130	-121	-33.7	-23.0	-21.0	86.14	4.72	1.66	0.38	0.50	0.13	0.11	n.d.	5.92	
		Long 42	J	770	-157	-132	-128	-32.9	-24.0	-21.2	90.52	4.96	1.50	0.32	0.39	0.10	0.08	n.d.	1.80	
		LS 17D	J	1680	-156	-130	-102	-32.7	-24.1	-21.6	90.66	5.47	1.46	0.19	0.33	0.07	0.04	n.d.	1.59	
		LS 12D	J	1744	-161	-132	-107	-32.9	-24.0	-20.9	89.94	5.87	1.72	0.30	0.43	0.09	0.08	n.d.	1.21	
		Long 75	J	1570	-158	-129	-110	-32.5	-23.7	-20.9	89.69	5.98	1.85	0.32	0.45	0.09	0.08	n.d.	1.24	
		Long 5	J	1150	-158	-126	n.d.	-34.5	-24.1	-21.4	85.57	6.48	2.81	0.63	0.77	0.19	0.16	n.d.	2.86	
		LS 3	J	1737	-164	-134	-111	-33.7	-24.3	-21.4	89.65	5.87	1.90	0.41	0.50	0.12	0.10	n.d.	0.96	
		DS 18	J	1889-1944.5	-164	-136	-121	-33.3	-24.8	-22.1	91.81	5.23	1.40	0.29	0.32	0.08	0.06	n.d.	0.48	
		DS 11	J	1856-1911	-157	-125	-107	-31.9	-23.9	-21.1	88.93	5.46	1.77	0.37	0.47	0.12	0.10	n.d.	2.36	
		DP 33	J	1117-1127	-160	-133	-124	-34.0	-24.6	-22.0	91.95	4.85	1.36	0.30	0.32	0.08	0.06	n.d.	0.89	
		DS 1	J	1897.9-1912.9	-160	-137	-119	-32.7	-25.2	-22.2	91.03	4.94	1.40	0.31	0.34	0.09	0.06	n.d.	1.49	
		DP 16	J	942.5-946.5	-155	-129	-119	-32.8	-24.5	-22.0	91.58	4.35	1.14	0.25	0.27	0.07	0.05	n.d.	2.07	
		LS27	J	1735.5-1758.5	-155	-136	n.d.	-34.1	-25.2	-22.6	84.80	11.92	1.31	0.27	0.23	n.d.	n.d.	0.04	1.32	This paper
		L9	J	667.5-676	-148	-120	n.d.	-34.6	-25.0	-22.8	91.96	3.99	1.56	0.22	0.21	n.d.	n.d.	0.04	1.90	
		DS8	J	2662-2672	-149	-136	-115	-34.1	-24.7	-22.1	89.57	5.50	2.08	0.32	0.24	n.d.	n.d.	0.04	2.12	
		MS1	J	3151.2-3175	-146	-141	-128	-33.4	-26.2	-22.9	92.36	4.12	1.55	0.21	0.26	n.d.	n.d.	0.05	1.36	
		CM602	K	1850.02-1862.02	-148	-143	n.d.	-34.0	-25.8	-23.4	95.37	2.67	0.81	0.19	0.08	n.d.	n.d.	0.09	0.69	
		CX455	J	2287-2406	-166	-135	-141	-36.4	-24.6	-21.7	88.89	7.14	2.35	0.37	0.39	n.d.	n.d.	0.01	0.71	
		CH127	T	4388.39-4644.87	-144	n.d.	n.d.	-32.1	-26.8	-27.0	97.09	0.94	0.22	n.d.	n.d.	n.d.	n.d.	1.11	0.45	
		HP1	J	1203.3-1211.7	-148	-142	-111	-36.8	-26.2	-23.8	94.59	3.36	1.23	0.03	0.02	n.d.	n.d.	0.10	0.64	
		X882	T	3383.58-3405.58	-152	-143	n.d.	-35.2	-24.3	-22.9	94.64	2.63	0.85	0.18	0.16	n.d.	n.d.	0.49	0.65	
Santanghu Basin		M17	J3q	512.4-524.2	-235	n.d.	n.d.	-36.4	-28.5	-30.1	2.00	0.22	0.48	0.21	0.27	n.d.	n.d.	0.22	52.56	This paper
		M18	J2x	1151-1154	-212	-173	-195	-35.1	-27.9	-27.9	65.40	3.99	3.44	1.01	1.38	0.28	0.54	0.05	21.69	
		M18	P1k	1423-1445	-214	-170	-182	-35.6	-28.2	-28.0	32.81	6.15	4.92	1.77	2.96	0.67	0.92	0.18	49.53	
		M8	P1k	1625-1644	-207	-169	-184	-35.3	-27.8	-25.5	72.88	8.25	6.47	1.35	2.16	0.66	0.16	0.16	7.75	
		M8	P1k	n.d.	-208	-216	n.d.	-35.0	-26.3	-26.8	73.07	8.18	6.05	1.19	1.87	n.d.	n.d.	0.24	8.79	
		M18	P1k	1326 - 1353	-216	-172	-214	-36.5	-27.5	-27.8	47.99	8.10	10.32	3.53	5.23	1.61	2.46	0.06	18.32	

Basin		Sample	Formation	Depth(m)	Hydrogen isotopic composition(‰)			Carbon isotopic composition(‰)			Gas chemical composition (%)									Data source
					δD_{CH_4}	$\delta D_{C_2H_6}$	$\delta D_{C_3H_8}$	$\delta^{13}C_{CH_4}$	$\delta^{13}C_{C_2H_6}$	$\delta^{13}C_{C_3H_8}$	C_1	C_2	C_3	iC_4	nC_4	iC_5	nC_5	CO_2	N_2	
		M8	J2t	721-726	-234	-168	-146	-38.1	-24.5	-25.2	89.71	5.16	2.03	0.64	n.d.	n.d.	n.d.	n.d.	n.d.	
		M8	J3q	535.0-543.4	-220	-159	-182	-38.7	-23.6	-24.6	70.95	3.75	1.13	0.29	n.d.	n.d.	n.d.	n.d.	n.d.	
		M8	J3q	337-367	-223	-157	-189	-37.9	-26.4	-23.3	77.40	3.45	1.05	0.30	0.12	0.04	0.02	0.32	17.33	
		M17	P1k	1515-1543	-220	-182	-188	-34.7	-27.9	-27.0	75.40	8.13	2.60	0.55	0.65	0.20	0.30	0.19	11.15	
		M18	P1k	1423-1445	-212	-144	-177	-33.8	-27.3	-26.8	62.80	7.39	5.20	2.05	1.70	0.61	0.50	0.01	17.90	
		M801	P1k	2029-2050	-215	-185	-184	-34.9	-28.0	-26.6	66.70	10.85	5.17	1.08	1.50	0.22	0.36	3.58	6.78	
Bohai Gulf Basin	Huanghua depression	ZH13-25l	E	n.d.	-215	-190	-184	-41.7	-29.5	-28.6	70.57	7.96	5.92	1.30	3.72	1.50	2.00	3.45	0.89	This paper
		ZH14-25l	E	n.d.	-212	-195	-183	-40.7	-29.9	-28.6	80.14	8.85	3.74	0.51	1.30	0.54	0.79	2.53	0.34	
		ZH21-23l	E	n.d.	-207	-195	-180	-43.6	-31.3	-28.8	76.33	9.71	4.94	0.72	1.77	0.61	0.88	2.45	1.17	
		ZH8Nm-H2	N	n.d.	-214	-133	n.d.	-44.2	n.d.	n.d.	79.21	0.41	4.36	1.61	5.19	2.51	3.40	n.d.	n.d.	
		ZH8Es-H1	E	n.d.	-218	-156	-111	-44.5	-27.8	-22.1	96.44	1.32	0.49	0.09	0.14	0.04	0.01	0.14	1.32	
		ZH8Es-H2	E	n.d.	-227	-164	-134	-43.3	-27.7	-22.9	92.49	1.87	1.14	0.32	0.86	0.53	0.74	0.19	0.82	
		ZH8Es-H3	E	n.d.	-219	-137	n.d.	-45.7	-29.8	n.d.	98.41	0.97	0.10	n.d.	0.01	n.d.	n.d.	0.14	0.37	
		GS20	Nm	1250.2-1531.8	-224	-148	n.d.	-42.4	-21.5	-17.2	97.05	0.52	0.05	0.01	0.02	0.01	n.d.	0.07	1.71	
		GS77	Ed_3	2616.8-2628.9	-205	-199	n.d.	-42.3	-29.7	-28.2	82.89	7.19	3.81	0.65	1.27	0.31	0.41	0.51	0.81	
		T30	Es_1	3126.5-3672.5	-181	-164	-204	-37.0	-26.2	-24.0	84.05	8.11	2.81	0.52	0.75	0.26	0.33	0.70	0.38	
		G24	Ng_3	2472-2503	-258	-197	-187	-46.0	-29.8	-28.4	85.17	5.50	3.49	0.68	1.13	0.32	0.26	0.21	1.14	
		G562	Ed_1	2180-2560	-211	-188	n.d.	-42.4	-29.2	-27.7	84.77	6.66	3.01	0.46	0.72	0.18	0.21	0.45	1.98	
		G561	Ed_3	2440.8-2517.0	-187	-172	-211	-38.2	-27.3	-25.4	83.15	8.06	3.27	0.57	0.96	0.29	0.37	0.22	0.76	
		G528	Ed_3	2540.8-2606.6	-190	-172	-162	-37.6	-27.3	-25.6	85.61	6.89	2.71	0.45	0.74	0.21	0.28	0.40	0.81	
		MG1	Es_1	3270.1-3284.3	-220	-171	-173	-44.9	-27.0	-26.1	77.17	9.51	4.73	0.97	1.40	0.54	0.65	0.23	0.69	
		GS12-18	E	3854.4-3871.3	-201	-194	-207	-40.4	-29.0	-26.7	80.52	8.57	3.86	0.66	1.41	0.39	0.60	1.00	0.72	
		GS14-18	E	3499.3-3763.6	-222	-206	-206	-43.7	-30.2	-29.8	84.77	6.05	3.68	0.50	1.38	0.29	0.41	1.08	0.79	
		QX24	Es_3	3062.2-3113.7	-246	-200	-185	-44.9	-27.7	-26.6	75.70	8.37	4.72	1.20	2.37	0.73	0.90	0.61	0.13	
		Q443	Es_1	2407.1-2440.6	-237	-198	-180	-47.3	-28.8	-27.6	77.79	7.70	4.55	0.85	2.02	0.54	0.77	0.27	1.85	
		X3-7-1	Ng	1045.0-1207.0	-220	-160	n.d.	-47.2	-26.4	-25.8	94.52	1.80	0.44	0.08	0.12	0.03	0.04	1.58	0.89	
		Q664	Es_3	2150.4-2215.0	-230	-180	-170	-44.0	-28.7	-25.2	89.01	3.54	1.56	0.42	0.83	0.34	0.32	0.27	1.24	
		B64-32	Ed	1907.1-1912.9	-230	-171	-193	-47.0	-26.9	-23.2	84.39	6.00	3.02	0.84	0.80	0.32	0.10	0.16	1.56	
		ZH19-1	Ed_1	2885.6-2994.1	-226	-206	-195	-43.2	-29.5	-28.6	77.65	7.68	4.03	0.73	1.70	0.52	0.81	0.41	1.33	
		ZH20-30	Ed_1	3096.5-3150.9	-234	-212	-237	-45.8	-29.8	-28.8	74.90	7.68	4.81	1.21	2.35	0.62	0.82	0.61	1.18	
		BH28	Es1	4328.9-4338.9	-178	-176	-151	-37.6	-27.6	-26.1	86.72	5.98	3.04	0.91	1.01	0.35	0.30	1.01	0.19	
		BH24	Ed3	3445.2-3450.8	-170	-161	-142	-36.8	-26.7	-25.0	86.47	6.94	3.03	0.43	0.73	0.12	0.13	0.10	1.92	
	Liaohe depression	N22-022	E	1893.8-1907.9	-240	-186	-163	-42.1	-26.4	-24.9	87.74	8.26	1.28	0.14	0.44	0.09	0.16	0.19	1.62	This paper
		N2721	E	1593.4-1620.4	-227	n.d.	n.d.	-43.4	n.d.	n.d.	98.40	0.20	n.d.	n.d.	n.d.	n.d.	n.d.	n.d.	1.34	
		C48-G84	E	2182.9-2363.8	-247	-206	-188	-42.4	-28.1	-26.7	82.07	12.02	1.74	0.22	0.56	0.08	0.09	0.45	2.75	
		Q2-22-3017	E	1404.5-2065.6	-221	n.d.	n.d.	-40.4	n.d.	n.d.	99.64	0.03	0.01	n.d.	0.02	0.01	0.02	0.04	0.21	
		Q2-22-208C	E	n.d.	-214	n.d.	n.d.	-43.9	n.d.	n.d.	98.97	0.34	0.02	n.d.	0.03	0.01	0.03	0.02	0.54	
		SH32-24	E	2351.0-2404.0	-208	-174	-165	-45.0	-28.8	-25.9	84.81	10.68	1.25	0.15	0.51	0.12	0.20	0.62	1.43	
		SH34-18	E	2909.8-2920.0	-210	-176	-165	-40.2	-27.0	-25.5	86.84	8.95	1.25	0.13	0.46	0.17	0.06	0.43	1.57	
		SH39-K12	E	2636.2-2888.6	-207	-169	-161	-40.5	-27.3	-25.9	85.53	9.82	1.28	0.17	0.51	0.13	0.20	0.78	1.53	
		SH36-16	E	2909.8-2920.0	-209	-162	-161	-39.6	-27.1	-25.3	82.20	7.91	4.55	0.65	1.95	0.60	0.94	0.34	0.09	
		SH9-5C	E	n.d.	-236	-180	-166	-48.9	-28.4	-24.5	88.18	8.40	0.62	0.27	0.47	0.19	0.21	0.70	0.82	
		F53-46	E	n.d.	-267	-208	-178	-44.3	-28.5	-25.1	85.57	10.13	1.39	0.20	0.46	0.08	0.11	0.10	1.93	
		R66	E	2286.6-2891.1	-213	-188	-155	-38.3	-28.6	-25.4	96.59	0.91	1.26	0.21	0.45	0.12	0.15	0.01	0.27	
		DA40	E	2079.1-2094.9	-191	-154	-131	-36.2	-26.1	-23.4	89.40	7.76	0.94	0.12	0.31	0.07	0.10	0.05	1.22	
		X140	E	1490.2-1498.8	-224	-130	n.d.	-43.2	-26.2	-16.1	97.33	1.04	0.04	0.09	0.01	n.d.	n.d.	0.05	1.41	
		XG7-H301	Ar	n.d.	-194	-166	-145	-37.2	-27.2	-24.7	62.65	4.76	0.56	0.06	0.14	0.02	0.03	0.15	31.17	
		XG7-5	Mz	3185.0-3243.4	-186	-165	-145	-36.3	-26.6	-24.5	63.39	4.63	0.70	0.12	0.28	0.07	0.12	0.07	30.16	
		MG1	Ar	3844.83-4081.02	-173	-142	-133	-31.0	-24.8	-23.8	91.77	4.80	0.70	0.12	0.26	0.06	0.10	0.16	2.00	
		H23	E	1700.4-1876	-235	-163	n.d.	-41.5	-26.5	-25.8	93.93	4.93	0.14	0.04	0.05	0.03	0.02	0.07	0.78	
		H105	E	1380-1383.4	-221	n.d.	n.d.	-44.0	n.d.	n.d.	99.51	0.10	n.d.	n.d.	n.d.	n.d.	n.d.	0.02	0.38	
		RQ2	E	1593.51661.4	-234	-193	n.d.	-49.4	-38.7	-27.2	98.63	0.80	0.05	0.01	0.01	n.d.	n.d.	0.04	0.46	
		R11	E	1415.9-1486.6	-231	-157	n.d.	-45.7	-26.6	-27.5	98.68	0.93	0.05	0.02	0.01	n.d.	0.01	0.01	0.28	
		H24	E	2287.3-2502.3	-224	n.d.	n.d.	-41.1	-26.0	-27.5	98.26	0.48	0.03	0.01	0.01	0.07	0.29	0.09	0.67	
		Y22	E	1934.6-2792	-255	-229	-181	-46.4	-31.1	-26.9	89.05	6.70	1.19	0.24	0.42	0.07	0.09	0.51	1.71	
		H9	E	2477.4-2997.6	-212	-176	n.d.	-40.1	-27.5	-25.3	87.27	9.53	1.16	0.09	0.24	0.02	0.03	0.21	1.45	
		H202	E	2767.8-3152	-250	-209	-106	-44.6	-29.5	-23.5	89.05	8.80	0.27	n.d.	0.02	0.02	0.09	0.85	0.83	
		OU25-21	E	2176-2270	-225	-199	-176	-38.6	-27.6	-25.9	90.57	5.09	1.27	0.20	0.38	0.06	0.08	0.12	2.20	
		J2-10-22	E	2103.9-2116.0	-224	-165	n.d.	-41.3	-28.1	-24.0	89.25	5.96	2.07	0.47	0.58	0.22	0.20	0.28	0.59	
		J323	E	3149.9-3184.8	-205	-156	n.d.	-40.2	-29.5	-28.5	66.91	9.56	9.08	1.95	4.09	1.24	1.34	3.12	2.05	
		J2-6-127	E	1415.2-1439.9	-219	n.d.	n.d.	-41.0	-23.4	-19.6	88.80	1.22	0.98	0.12	0.25	0.03	0.03	5.63	2.45	
		CG5	Ar	4447.3-4529	-200	-157	n.d.	-42.7	-27.4	-24.8	79.26	9.40	4.22	0.71	1.15	0.28	0.28	1.82	2.35	
		CG2	Ar	4103-4240.4	-202	-164	n.d.	-43.3	-27.7	-25.1	78.09	9.82	4.46	0.70	1.11	0.26	0.25	1.49	2.98	
		CG1c	Ar	4584-4634	-206	-170	n.d.	-41.6	-28.4	-21.0	81.93	6.96	0.55	0.54	n.d.	0.14	0.16	1.14	4.35	
		L64	E	2042-2174	-240	-174	n.d.	-48.9	-31.2	-29.8	87.62	5.54	3.10	0.49	0.89	0.24	0.23	0.18	1.39	
		SH227	E	3938.7-3987.2	-200	-173	n.d.	-39.4	-28.4	-25.9	83.19	7.58	1.30	0.11	0.20	0.05	0.06	0.89	5.06	
		M70-1	E	n.d.	-229	-188	n.d.	-45.4	-31.1	-28.0	82.46	8.81	4.59	0.58	1.09	0.27	0.28	1.50	0.13	
		M256	E	n.d.	-231	-195	n.d.	-45.7	-30.4	-27.8	84.75	7.89	4.34	0.52	0.95	0.18	0.16	0.76	0.25	
		M726c	Ar	n.d.	-219	n.d.	n.d.	-45.8	-26.7	-25.6	91.90	0.52	0.81	0.54	0.80	0.38	0.31	0.26	3.90	
		X86c	Ar	2073.2-2486.0	-193	-164	n.d.	-37.2	-27.0	-25.9	85.70	7.14	3.16	0.84	1.04	0.29	0.28	0.45	0.83	
		X4-20	E	2278-2351.6	-223	-159	n.d.	-42.0	-27.0	-26.8	84.51	5.46	3.84	1.12	1.57	0.59	0.57	0.70	1.02	
		XQ9	Ar	3214.0-3258.0	-193	-173	n.d.	-36.8	-27.6	-25.8	85.51	7.37	3.31	0.77	0.90	0.22	0.20	0.19	1.31	
		XQ8	Ar	2967.1-3022.1	-190	-171	n.d.	-36.6	-27.4	-25.6	83.49	9.00	3.57	0.77	0.85	0.21	0.26	0.46	0.80	
		MG7	Ar	n.d.	-173	-160	n.d.	-31.9	-26.2	-25.7	85.21	5.08	2.80	1.01	1.29	0.60	0.63	0.28	2.12	
		T601	Ar	n.d.	-197	-143	n.d.	-38.6	-27.6	-25.3	88.74	3.98	2.36	0.61	0.84	0.31	0.29	0.45	1.87	
		W609	Ar	n.d.	-235	n.d.	n.d.	-42.3	-29.9	-26.7	91.80	3.71	1.83	0.35	0.47	0.14	0.12	0.20	1.15	
		ZG1	Ar	n.d.	-189	-138	n.d.	-38.1	-25.1	-24.5	81.38	6.93	3.81	2.18	1.43	0.48	0.38	0.24	2.39	
		QG63	Ar	n.d.	-229	n.d.	n.d.	-42.6	-30.1	-26.9	75.54	11.27	6.17	1.04	2.15	0.58	0.74	1.34	0.42	
		SH100	E	3252-3271	-202	-166	n.d.	-41.3	-28.3	-26.5	74.55	10.17	4.62	0.72	1.43	0.34	0.35	2.95	4.15	
		SH208	E	3441.5-3474.5	-201	-169	n.d.	-41.4	-28.5	-26.6	73.21	12.37	6.41	1.04	2.18	0.57	0.64	2.28	0.66	
		SH118	E	3385.4-3396.4	-200	-178	n.d.	-39.5	-28.9	-27.3	78.68	9.51	4.78	0.86	1.80	0.56	0.66	2.04	0.24	

Associate Editor—**Maowen Li**

References

Barker, J.F., Pollock, S.J., 1984. The geochemistry and origin of natural gases in Southern Ontario. Bulletin of Canadian Petroleum Geology 32, 313–326.

Bigeleisen, J., 1965. Chemistry of isotopes. Science 147, 463–471.

Cai, C.F., Hu, G.Y., He, H., Li, J., Li, J.F., Wu, Y.S., 2005. Geochemical characteristics and origin of natural gases and thermochemical sulphate reduction in Ordovician carbonates in the Ordos Basin. Journal of Petroleum Science and Technology 48, 209–226.

Chen, A.D., 1994. Origin and migration of natural gases in Ordovician reservoir in Shan Gan Ning Basin Central Gas field (in Chinese with English abstract). Acta Petrolei Sinica 15, 1–10.

Coleman, D.D., Risatti, J.B., 1981. Fractionation of carbon and hydrogen isotopes by methane-oxidizing bacteria. Geochimica et Cosmochimica Acta 45, 1033–1037.

Dai, J.X., 1990. Characteristics of hydrogen isotopes of paraffinic gas in China (in Chinese with English abstract). Petroleum Exploration and Development 17, 27–32.

Dai, J.X., 1992. Identification and distinction of various alkane gases. Science in China (Series B) 35, 1246–1257.

Dai, J.X., 1993. Characteristics of carbon and hydrogen isotopes of natural gases and their discriminations (in Chinese with English abstract). Natural Gas Geoscience 4, 1–40.
Dai, J.X., Zou, C.N., Li, J., 2009. Carbon isotopes of Middle-Lower Jurassic coal-derived alkane gases from the major basins of northwestern China. International Journal of Coal Geology 80, 124–134.
Dai, J.X., Li, J., Luo, X., Zhang, W.Z., Hu, G.Y., Ma, C.H., Guo, J.M., Ge, S.G., 2005. Stable carbon isotope compositions and source rock geochemistry of the giant gas accumulations in the Ordos Basin, China. Organic Geochemistry 36, 1617–1635.
Dai, J.X., Xia, X.Y., Li, Z.S., Coleman, D.D., Dias, R.F., Gao, L., Li, J., Deev, A., Li, J., Dessort, D., Duclerc, D., Li, L.W., Liu, J.Z., Schloemer, S., Zhang, W.L., Ni, Y.Y., Hu, G.Y., Wang, X.B., Tang, Y.C., 2012a. Inter-laboratory calibration of natural gases round robins for δ^2H and $\delta^{13}C$ using off-line and on-line techniques. Chemical Geology 310–311, 49–55.
Dai, J.X., Ni, Y.Y., Zou, C.N., 2012b. Stable carbon and hydrogen isotopes of natural gases sourced from the Xujiahe Formation in the Sichuan Basin, China. Organic Geochemistry 43, 103–111.
Feng, Q., Geng, A.S., Liao, Z.W., Zhang, X.L., 2007. Carbon and hydrogen isotopic compositions of coal-genetic natural gases and their applications in accumulation in Upper Paleozoic, Ordos Basin (in Chinese with English abstract). Geochimica 36, 261–266.
Guan, D.F., Zhang, W.Z., Pei, G., 1993. Oil–gas sources of Ordovician reservoir in gas field of central Ordos Basin (in Chinese with English abstract). Oil and Gas Geology 14, 191–199.
Hao, S.S., Gao, Y.B., Huang, Z.L., 1997. Characteristics of dynamic equilibrium for natural gases migration and accumulation of the gas field in the center of the Ordos Basin. Science in China, Series D 2, 11–15.
Hilkert, A.W., Douthitt, C.B., Douthitt, C.B., Schluter, H.J., Brand, W.A., 1999. Isotope ratio monitoring gas chromatography/mass spectrometry of D/H by high temperature conversion isotope ratio mass spectrometry. Rapid Communications in Mass Spectrometry 13, 1226–1230.
Hu, G.Y., Li, J., Shan, X.Q., Han, Z.X., 2010. The origin of natural gases and the hydrocarbon charging history of the Yulin gas field in the Ordos Basin, China. International Journal of Coal Geology 81, 381–391.
Huang, D.F., Xiong, C., Yang, J., 1996. Gas source discrimination and natural gases genetic types of Central Gas Field in Ordos Basin (in Chinese with English abstract). Natural Gases Industry 16, 1–5.
Jin, H., Yang, W., Xie, W.R., Zhao, X.Y., Xie, Z.Y., Shi, Z.S., 2010. Application of clay minerals in sedimentary environmental research of Xujiahe Formation in Sichuan Basin (in Chinese with English abstract). Journal of Oil and Gas Technology 32, 17–21.
Lewan, M.D., 1997. Experiments on the role of water in petroleum formation. Geochimica et Cosmochimica Acta 61, 3691–3723.
Li, M.W., Huang, Y., Obermajer, M., Jiang, C., Snowdon, L.R., Fowler, M.G., 2001. Hydrogen isotopic compositions of individual alkanes as a new approach to petroleum correlation: case studies from the Western Canada Sedimentary Basin. Organic Geochemistry 32, 1387–1399.
Li, X.Q., Hu, G.Y., Li, J., Hou, D.J., Dong, P., Song, Z.H., Yang, Y.F., 2008. The characteristics and sources of natural gases from Ordovician weathered crust reservoirs in the Central Gas Field in the Ordos Basin. Chinese Journal of Geochemistry 27, 109–120.
Lin, L.B., Chen, H.D., Jiang, P., Hu, X.Q., Ji, X.T., Ye, L.M., 2006. Sedimentary facies and litho-paleogeographic evolution of the Upper Triassic Xujiahe Formation in West Sichuan foreland basin (in Chinese with English abstract). Journal of Chendou University of Technology 33, 376–383.
Lin, X., 2011. Application of paleo-oxygen facies analysis to the sedimentary environment research of the Paleogene Shahejie Formation in the South Qikou sag, Huanghua depression, China (in Chinese with English abstract). Journal of Chendou University of Technology 38, 651–655.
Liu, Q.Y., Chen, M.J., Liu, W.H., Li, J., Han, P.L., Guo, Y.R., 2009. Origin of natural gases from the Ordovician paleo-weathering crust and gas-filling model in Jingbian gas field, Ordos Basin, China. Journal of Asian Earth Science 35, 74–88.
Liu, W.H., Chen, M.J., Guan, P., Zheng, J.J., Jin, Q., Li, J., Wang, W.C., Hu, G.Y., Xia, Y.Q., Zhang, D.W., 2007. Ternary geochemical-tracing system in natural gases accumulation. Science in China (Series D) 50, 1494–1503.
Liu, W.H., Xu, Y.C., 1999. A two-stage model of carbon isotopic fractionation in coal gas (in Chinese with English abstract). Geochimica 7, 359–366.
Liu, Q.Y., Dai, J.X., Li, J., Zhou, Q.H., 2008. Hydrogen isotope composition of natural gases from the Tarim Basin and its indication of depositional environments of the source rocks. Science in China (Series D) 51, 300–311.
Mastalerz, M., Schimmelmann, A., 2002. Isotopically exchangeable organic hydrogen in coal relates to thermal maturity and maceral composition. Organic Geochemistry 339, 21–931.
Qin, S.F., Dai, J.X., Liu, X.H., 2007. The controlling factors of oil and gas generation from coal in the Kuqa Depression of Tarim Basin, China. International Journal of Coal Geology 70, 255–263.
Sessions, A.L., Burgoyne, T.W., Schimmelmann, A., Hayes, J.M., 1999. Fractionation of hydrogen isotopes in lipid biosynthesis. Organic Geochemistry 30, 1193–1200.
Schimmelmann, A., Boudou, J.P., Lewan, M.D., Robert, P.W., 2001. Experimental controls on D/H and $^{13}C/^{12}C$ ratios of kerogen, bitumen and oil during hydrous pyrolysis. Organic Geochemistry 32, 1009–1018.
Schimmelmann, A., Lewan, M.D., Wintsch, R.P., 1999. D/H isotope ratios of kerogen, bitumen, oil and water in hydrous pyrolysis of source rocks containing kerogen types I, II, IIS, III. Geochimica et Cosmochimica Acta 63, 3751–3766.
Schoell, M., 1983. Genetic characterization of natural gases. American Association of Petroleum Geologists Bulletin 67, 2225–2238.
Schoell, M., 1988. Multiple origins of methane in the earth. Chemical Geology 71, 1–10.
Schoell, M., 1984. Recent advances in petroleum isotope geochemistry. Organic Geochemistry 6, 645–663.
Schoell, M., 1980. The hydrogen and carbon isotopic composition of methane from natural gases of various origins. Geochimica et Cosmochimica Acta 44, 649–661.
Shen, P., Xu, Y., 1993. Isotopic compositional characteristics of terrigenous natural gases in China. Chinese Journal of Geochemistry 12, 14–24.
Shi, B.G., Shen, P., Wang, X.F., Zhen, J.J., 2012. Groundbreaking gas source rock correlation research based on the application of a new experimental approach for adsorbed gas. Chinese Science Bulletin 57, 4746–4752.
Shouakar, S.O., Drimmie, R., Morrison, J., Frape, S.K., Heemskerk, A.R., Mark, W.A., 2000. On-line D/H analysis for water, natural gases and organic solvents by manganese reduction. Analytical Chemistry 72, 2664–2666.
Stahl, W., Boigk, H., Wollanke, G., 1977. Carbon and nitrogen isotope data of Upper Carboniferous and Rotliegend natural gases from North Germany and their relationship to the maturity of the organic source material. Advances in Organic Geochemistry 3, 539–559.
Stahl, W.J., Carey, B.D., 1975. Source-rock identification by isotope analyses of natural gases from fields in the Val Verde and Delaware basins, West Texas. Chemical Geology 16, 257–267.
Wang, X.F., Liu, W.H., Xu, Y.C., Zheng, J.J., 2011. Influences of water media on the hydrogen isotopic composition of natural gases/methane in the processes of gaseous hydrocarbon generation and evolution. Science in China (Series D) 54, 1318–1325.
Wang, X.F., Liu, W.H., Xu, Y.C., Zheng, J.J., Zhang, D.W., Shi, B.G., 2008. Pyrolytic simulation experiments on the role of water in natural gases generation from coal. International Journal of Coal Geology 75, 105–112.
Whiticar, M.J., Faber, E., Schoell, M., 1986. Biogenic methane formation in marine and freshwater environments—CO_2 reduction vs. acetate fermentation—isotopic evidence. Geochimica et Cosmochimica Acta 50, 693–709.
Whiticar, M.J., 1999. Carbon and hydrogen isotope systematics of bacterial formation and oxidation of methane. Chemical Geology 161, 291–314.
Whiticar, M.J., 1996. Stable isotope geochemistry of coals, humic kerogens and related natural gases. International Journal of Coal Geology 32, 191–215.
Xu, Y.C., 1994. Origin Theory and Application of Natural Gases (in Chinese). Science Press, Beijing, 1–414.
Xu, Y.C., Wang, Z.Y., Wang, X.F., Zheng, J.J., Du, H.Y., 2006. Low-mature gases and typical low-mature gas fields in China. Science in China (Series D) 49, 938–946.
Xu, Y.C., Wang, X.F., Shi, B.G., 2009. Low-mature gases and their resource potentiality. Chinese Journal of Geochemistry 28, 231–238.
Yeh, H., Epstein, S., 1981. Hydrogen and carbon isotopes of petroleum and related organic matter. Geochimica et Cosmochimica Acta 45, 753–762.
Zhang, S.C., Mi, J.K., Liu, L.H., Tao, S.Z., 2009. Geological features and formation of coal-formed tight sandstone gas pools in China: cases from Upper Paleozoic gas pools, Ordos Basin and Xujiahe Formation gas pools, Sichuan Basin (in Chinese with English abstract). Petroleum Exploration and Development 36, 320–330.
Zhang, W.Z., Pei, G., Guan, D.S., 1993. Carbon isotopic distribution characteristics of light hydrocarbon monomeric series of crude oils in the Ordos Basin. Chinese Science Bulletin 38, 64–68.